Journal Pre-proof

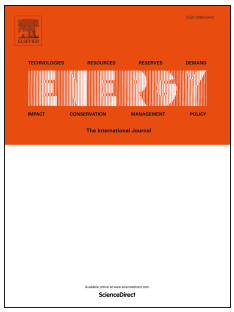

Deploying Bioenergy for Decarbonizing Malaysian Energy Sectors and Alleviating Renewable Energy Poverty

Muhammad Nurariffudin Mohd Idris, Haslenda Hashim, Sylvain Leduc, Ping Yowargana, Florian Kraxner, Kok Sin Woon

PII: S0360-5442(21)01215-9

DOI: https://doi.org/10.1016/j.energy.2021.120967

Reference: EGY 120967

To appear in: *Energy*

Received Date: 31 January 2021

Revised Date: 21 April 2021

Accepted Date: 14 May 2021

Please cite this article as: Mohd Idris MN, Hashim H, Leduc S, Yowargana P, Kraxner F, Woon KS, Deploying Bioenergy for Decarbonizing Malaysian Energy Sectors and Alleviating Renewable Energy Poverty, *Energy*, https://doi.org/10.1016/j.energy.2021.120967.

Credit Author Statement

Muhammad Nurariffudin Mohd Idris: Data curation, Investigation, Methodology, Software, Writing - original draft

Haslenda Hashim: Data curation, Funding acquisition, Supervision, Validation, Writing - review & editing

Sylvain Leduc: Conceptualization, Methodology, Software, Supervision, Validation, Writing - review & editing

Ping Yowargana: Conceptualization, Supervision, Writing - review & editing

Florian Kraxner: Conceptualization, Funding acquisition

Kok Sin Woon: Writing - review & editing

Deploying Bioenergy for Decarbonizing Malaysian Energy Sectors and Alleviating Renewable Energy Poverty

Muhammad Nurariffudin Mohd Idris[a], Haslenda Hashim[a,*], Sylvain Leduc[b], Ping Yowargana[b], Florian Kraxner[b], Kok Sin Woon[c]

[a]Process Systems Engineering Centre (PROSPECT), School of Chemical and Energy Engineering, Faculty of Engineering, Universiti Teknologi Malaysia, 81310 UTM Johor Bahru, Skudai, Johor, Malaysia

[b]Ecosystems Services and Management (ESM), International Institute for Applied Systems Analysis (IIASA), Schlossplatz 1, A-2361 Laxenburg, Austria

[c]School of Energy and Chemical Engineering, Xiamen University Malaysia, Jalan Sunsuria, Bandar Sunsuria, 43900 Sepang, Selangor, Malaysia

*Corresponding author: haslenda@utm.my (H. Hashim).

Abstract

Due to the capital cost of co-firing being lower than other biomass technologies, the transformation of coal plants into co-firing facilities can potentially minimize the bioenergy cost needed to meet energy decarbonization targets. This study analyzes the impact of the co-deployment of co-firing and dedicated biomass technologies in contributing to the bioenergy cost reduction for country-level energy systems using a spatio-temporal techno-economic optimization model. Malaysia is used as a case in the analysis. Different scenarios were developed to assess the robustness of the cost reduction potential under the impact of incremental CO_2 reduction targets and supply chain cost parameter variations. Our results suggest that the multi-sectoral deployment of bioenergy in energy systems is key to meeting decarbonization targets at the national scale. By also considering co-firing in the biomass technological pathway, up to 27% of bioenergy cost reduction can be enabled in the baseline case. The decrease in the supply chain cost parameter values further enhances the cost reduction potential; bioenergy costs can be reduced up to threefold. The findings have shown that developing countries such as Malaysia can benefit from the use of their rich agricultural resources to cost-effectively alleviate renewable energy poverty.

Keywords:
Bioenergy; renewable energy; decarbonization; spatial analysis; optimization; oil palm biomass.

Highlights

- Biomass co-firing plays an important role in delivering energy decarbonization
- Multi-sectoral deployment helps to improve bioenergy production efficiency
- More bioenergy investments are needed when co-firing is unavailable
- The capital cost savings provided by co-firing reduce energy decarbonization costs
- Changes in supply chain cost parameter values affect the cost reduction potential

1.0 Introduction

For developing countries that are dependent on agricultural resources, opportunities arise to mobilize biomass wastes generated from agricultural production activities for utilization as feedstock for energy production. Biomass co-firing with coal has been viewed in many studies as a low-cost renewable energy option for mitigating coal-based CO_2 emissions due to the low capital investment associated with the integration of bioelectricity production in the existing power generation infrastructure [1-4]. However, without substantial plant modification, co-firing can only replace up to 20% of the existing coal plant capacity, if provided with the use of densified biomass feedstock [5]. This limits the opportunity for co-firing to harness the maximum biomass potential that could be deployed within a country. To make full use of the biomass potential available while replacing a significant share of the fossil fuels in the energy mix, co-firing can also be deployed alongside dedicated biomass technologies, such as bioelectricity, bioheat and biofuels, which are not restricted by the availability of the existing power generation infrastructure.

Coupling the deployment of biomass retrofit in the existing fossil fuel assets with dedicated biomass technologies, which are typically more capital intensive [6], could potentially result in capital cost savings that would lead to a reduction in the overall cost of energy systems. This fact was quantitatively presented in few recent studies, e.g., Keller et al. [2] found that in the

projected Alberta's electricity system pathway, not adopting biomass retrofit technology in the existing power plant increases the total system cost by 5%. Meanwhile, Bui et al. [7] showed that in the projected biomass-based negative emission pathway, adopting biomass retrofit technology in the existing UK-based power plants results in improved profitability of the energy systems. However, these analyses were based on biomass retrofit pathways that adopted a 100% conversion of coal-fired units to biomass-fired units. A critical question arises: would a co-firing plant with a lower biomass-to-coal blending ratio (< 20%) still provide substantial capital cost savings compared to a 100% biomass retrofit plant? It is important to address this question to inform energy systems planners and policymakers when they make decisions on whether to focus on pursuing new policies that allow co-firing in the existing power plants [8,9] or to focus on strengthening current policies that promote dedicated biomass technologies and other renewables [10,11]. This insight is important because, in several developing countries, policies promoting co-firing remain unavailable, although policies promoting renewables are already incorporated in national policies [1]. Thus, to inform the priority-setting of the national energy policy, a detailed assessment regarding these issues is needed at the country scale. To the best of the authors' review, the existing comparative assessments of co-firing and dedicated biomass technologies have been conducted mainly at the plant level [6,12-14]. The insights derived from these previous works, however, are still inadequate to fully characterize the impact of co-firing on the cost-reduction of dedicated biomass technologies to decarbonize the energy sectors at the system level.

The deployment of co-firing has generally been evaluated individually rather than interdependently with dedicated biomass technologies in previous assessments [15-19]. Since various biomass conversion technologies are available, a suitable pathway for the co-deployment of co-firing and dedicated biomass technologies needs to be determined from a large array of possible supply chain configurations. Optimization models were often used in previous research to find the optimal design of the biomass supply chain [20]. In such models, the usual objective is to find the minimum cost (or emission) of the studied biomass pathway, at different system scales, e.g., district level [21-23], province/state level [24-26], national level [7,27-29], regional level [30-32], and continental level [33-35]. By using these models, multiple decisions, such as locating biomass feedstock supply sites [36,37], production sites [29,30] and energy demand sites

[31,33], and determining the required scales of the technological deployments [33-35], can be figured out simultaneously [20]. Despite the availability of existing optimization models capable of handling sophisticated biomass supply chain designs, a limited number of specialized bioenergy models exist that can capture sectoral disaggregation of the supply chains, in which techno-economic variables of certain supply chain activities are indexed according to their respective end-use demand sectors (such as Refs. [38,39]). This is a very important feature to include in an optimization model, as it captures the cross-sectoral impact of a wide range of biomass applications in multiple energy sectors. Durusut et al. [38] showed that the use of a model with multi-sectoral features can benefit policymakers in need of decision support when assessing the synergies between multiple policy goals and bioenergy initiatives in energy sectors. For instance, the models can be used to assess how a policy intervention implemented in one sector affects the policy goals in another. In this way, if conflict arises between the policy goals, the use of decision support tools can inform policymakers on the synchronization of those multiple policies. Clancy et al. [39] further showed that policies promoting the deployment of bioenergy in either one of the energy sectors affect the choice of technologies and the overall level of emission reduction delivered, using Ireland as a case study. The study highlighted that a policy supporting biomass utilization in the power sector limits the CO_2 reduction contribution by the heat sector, since both sectors majorly compete for national biomass resources to produce bioenergy. Although the works mentioned [38,39] showed the importance of incorporating a multi-sectoral perspective in assessing the bioenergy deployment, they did not illustrate the impact of capital cost savings on the reduction in bioenergy costs that could have been provided by co-firing. Moreover, these works did not properly account for the spatial effects of biomass technology deployment in long-term bioenergy scenarios. The geographical scope covered (i.e., country scale) was treated as a single zone, without accounting numerous spatial nodes allocated within the zone. Because of this aggregation, these modeling works did not have the granularity to generate location-specific insights related to the deployment of biomass technologies and co-firing, such as resource allocation [32,33], pre-processing depot localization [25,30], bioenergy plant localization [29,30], coal plant retrofit localization [31,40], and infrastructure network expansion [34,35], all of which are important to inform policy decisions.

Given the gaps in the literature, this study seeks to provide insights into the implications of deploying dedicated bioenergy technologies, with and without co-firing, on the costs of decarbonizing multiple energy sectors and the associated infrastructural requirements using a spatially-explicit techno-economic optimization model that combines the applications of Geographical Information Systems (GIS) and energy systems modeling. A key strength of this model is the endogenous representation of the supply chain, involving logistics, trades, conversions and demand competitions at specific bioenergy plant locations co-located with the locations of agricultural mills and clustered by spatial grid cells, which then translates into a higher-level system representation at the national or regional scale. Furthermore, this model associates multi-sectoral and high spatial resolution features covering a long-term planning timeframe until 2050, while also adopting features such as plant location-allocation, transmission network infrastructure interconnections, and different bioenergy pre-processing/conversion options for establishing the optimal bioenergy supply chain configurations. The model is applied to the case of the Malaysian bioenergy industry. The selection of Malaysia as the case study country for this assessment is based on two main criteria, namely its electricity mix and biomass availability. Since coal is projected to dominate the fuel share of Malaysia's electricity generation for the next few decades [41], co-firing can be deployed as a feasible renewable energy option in this country, considering the increasing capacity of coal-fired power plants. As both co-firing and dedicated bioenergy options require biomass as feedstock to produce bioenergy outputs, Malaysia's position among the largest global palm oil producers [42] suggests an opportunity to leverage the potential biomass supply. Although the model parameters employed in this study were customized to suit the bioenergy supply chain structure of Malaysia, the generalizable methodology and insights derived from this assessment are readily applicable to other countries or regions facing similar challenges.

Several objectives were defined in this study: 1) To identify the rates of cost reduction that can be enabled from deploying co-firing with dedicated biomass technologies, 2) To evaluate the technological and infrastructural requirements of deploying bioenergy predominantly from palm oil sources in the multiple energy sectors at the national scale; and 3) To assess the robustness of the bioenergy deployment with and without co-firing in meeting energy decarbonization targets under different supply chain cost parameter variations. Specifically, this

study aims to identify the technological transition required in the long term to achieve the national CO_2 reduction goals in line with the international climate policy, based on configuring the cost-optimal pathway that incorporates the production of bioenergy predominantly from palm oil-based sources with and without bioenergy retrofits in the existing coal plants. Aside from informing the ongoing initiatives and policies on fossil fuels mitigations and emission reductions, the techno-economic insights generated from this paper can also help to inform industrial actors on the best strategies to promote a sustainable bio-based economy based on improving the resource efficiency of the agricultural sectors through the use of biomass for bioenergy purposes. The insights can also help to inform developing countries with rich agricultural resources, such as Malaysia, on the strategies to alleviate renewable energy poverty in their energy sectors.

2.0 Methodology

2.1 Modeling approach

Malaysia's energy decarbonization pathway for the power, heat and transport sectors is modeled using the BeWhere Malaysia model [43]. The model was built based on the core version of the BeWhere model [44,45] developed at the International Institute for Applied Systems Analysis (IIASA). The BeWhere Malaysia model is a multi-sectoral, partial-equilibrium, mixed-integer linear programming model that determines the least-cost decarbonization pathway of energy systems at the national scale at a spatial resolution of 25 km x 25 km, covering a planning period of 2020–2050 (discretized into five-year time steps and two-month sub-annual time steps). Each spatial grid-cell contains area-specific information such as the types, rates, and costs of resources collected, stored, and processed; the demands of feedstock and bioenergy products; the types, capacities, and costs of bioenergy technologies; the distances, rates, and costs of resources transported; the infrastructure network extended; and the CO_2 emissions of all supply chain activities. Other features of the model include the optimal configuration of energy supply chain structure that suits an agricultural bioenergy supply chain based predominantly on palm oil sources, as well from paddy and livestock sources; the optimal planning of the feedstock and intermediate product storages; the optimal selection of pre-processing technologies that provide the use of upgraded feedstock, such as biomass pellets, biomethane and compressed biomethane (BioCNG); the optimal selection of conversion technologies for producing bioenergy products

such as bioelectricity, bioheat and biofuel; the optimal transportation of feedstock, intermediates and bioenergy products from the supply points to the demand points; and the optimal infrastructure network deployment comprised of the extension of power transmission lines from existing mills to substations and the extension of steam pipeline to the industrial areas. The model is written in GAMS and solved using the solver CPLEX. The description of the mathematical formulation of the BeWhere Malaysia model, together with the input datasets, is available online [46]. The overall structure of the BeWhere Malaysia model is illustrated in Fig. 1.

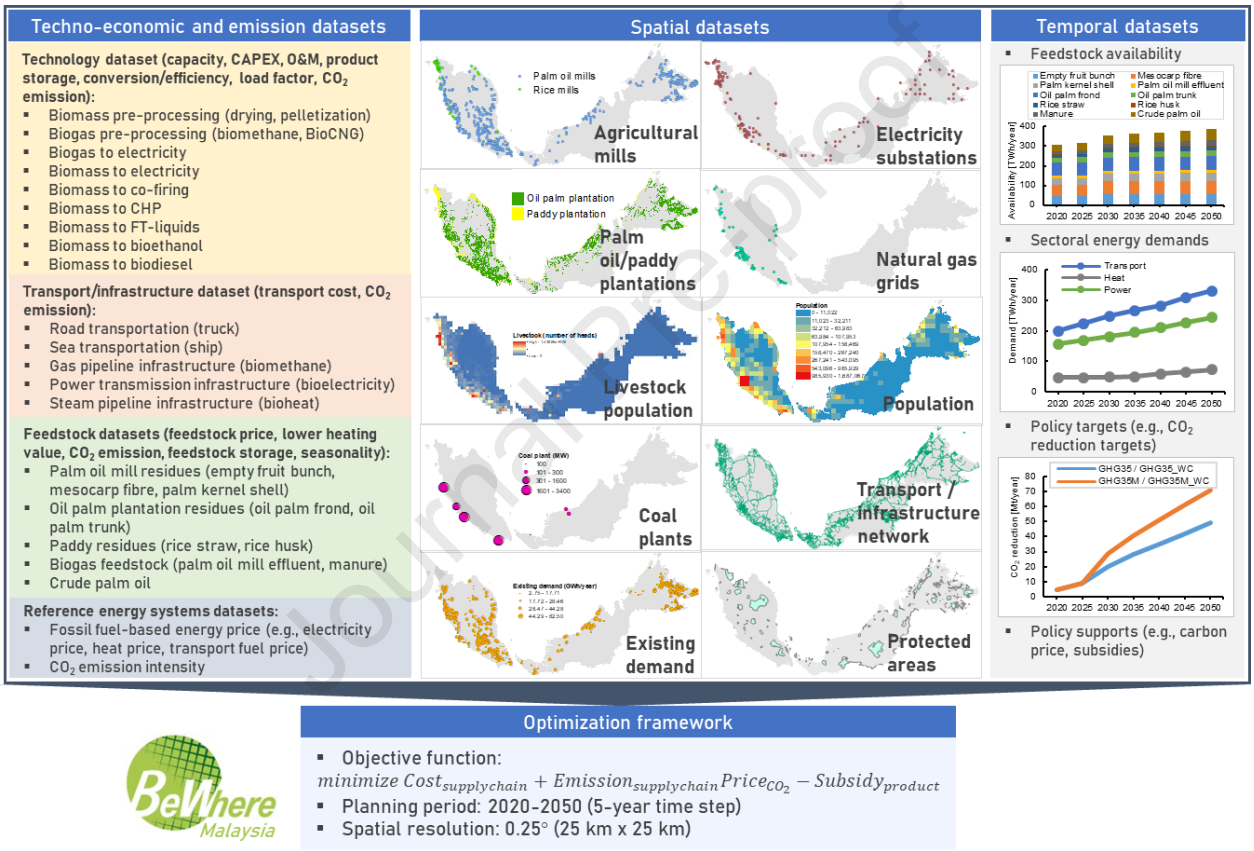

Fig. 1: The overall structure of the BeWhere Malaysia model. Four types of datasets are incorporated as inputs into the model, categorized as techno-economic datasets, emission datasets, spatial datasets, and temporal datasets. The energy supply chain structure of the model is designed to suit an agricultural bioenergy supply chain pathway predominantly based on palm oil resources. The model configures the optimal decarbonization pathway by determining the least-cost energy supply chain configuration while satisfying the annual CO_2 reduction targets as a constraint.

2.2 Bioenergy supply chain

The bioenergy supply chain structure in the model considers two processing stages, namely the pre-processing of feedstock into intermediate products and the conversion of feedstock and intermediate products into bioenergy products, as illustrated in Fig. 2. The feedstock is initially collected from the supply locations (e.g., palm oil mills, rice mills, oil palm plantations, paddy plantations, livestock farms). The feedstock may be stored for utilization in the subsequent sub-annual periods or directly transported to conversion plants or pre-processing plants while satisfying the demands for existing energy uses. The pre-processing of the feedstock may be performed to increase its energy density by converting it into an intermediate product (e.g., biomass pellets, biomethane, BioCNG). The intermediate product is then either stored for utilization in the subsequent sub-annual periods or transported to conversion plants for further conversion into bioenergy products or transported to coal plants for co-firing.

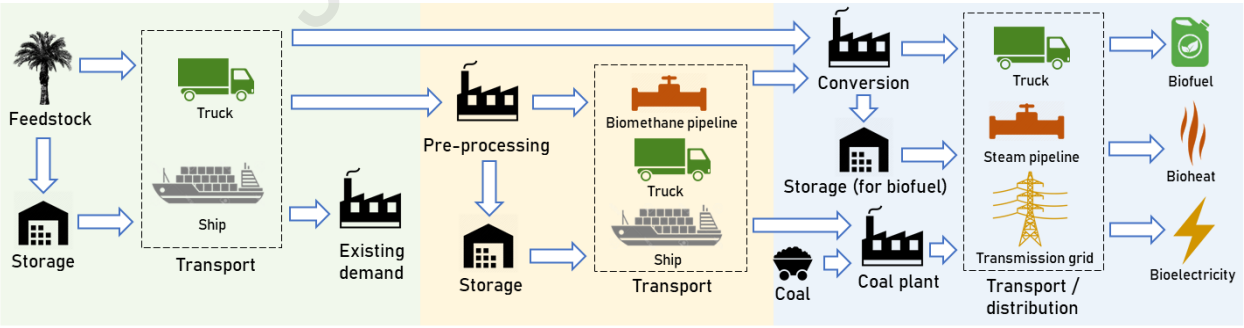

Fig. 2: The bioenergy supply chain structure adopted in BeWhere Malaysia.

Several transportation modes are considered in the model, including road transportation, sea transportation, pipeline transportation, and power grid transmission. For road transportation, truck is used to transport feedstock, intermediate product, and bioenergy product from the supply

points to the destinations. For sea transportation, ships are used to transport feedstock and intermediate product from seaports to the destinations. The majority of the feedstock is allowed to be transported using trucks or ships but an exception was made for palm oil mill effluent (POME), which is only allowed to be used onsite due to its slurry characteristic which makes it difficult to be transported using truck. However, POME can also be consumed in other locations if processed into biomethane or BioCNG. To deliver the biomethane into conversion facilities, a compressor unit of 20 psig operating pressure and an 8-inch pipe diameter pipeline are needed [47]. The production of bioelectricity requires the extension of power transmission lines from existing agricultural mills to electricity substations with capacities greater than 100 kV [34], whereas the production of bioheat requires the extension of a steam pipeline with a 6-inch pipe diameter to the industrial demand points [48]. The form of transport and the corresponding distances are obtained from spatial data using the network analysis tool in the ArcGIS software. The cost and CO_2 emission network for road transport, sea transport, pipeline transport, and power transmission are established through the interconnections of each of the associated spatial grid cells, as illustrated in Fig. 3. The parameters employed for establishing the transport networks, costs, and CO_2 emissions in ArcGIS are compiled in Table 1 and Table 2.

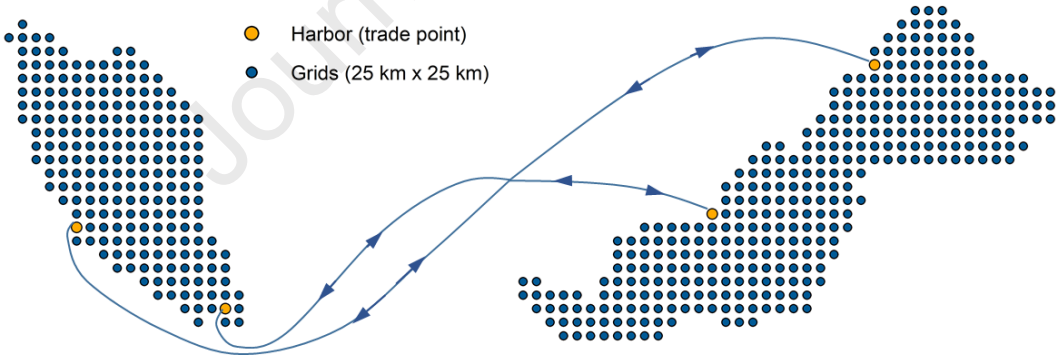

Fig. 3: Spatial grid cells covering the national administrative boundaries of Malaysia.

Table 1: Cost and emission parameters for road and sea transportation.

Transport parameters	Unit	Truck[a]	Ship[b]
Loading/unloading cost	USD/t	2.5	6.7
Transport cost	USD/t.km	0.05680	0.00131
Emission	gCO2/t.km	116	7

Fuel consumption[c]	L/vehicle.km	0.278	15.760

[a]Cost and emission parameters were calculated based on the parameters adapted from How et al. [49].

[b]Cost and emission parameters were calculated based on the parameters adapted from Rentizelas and Li [50].

[c]Transport fuel cost was calculated based on the annual fuel price of each planning period.

Table 2: Cost parameters for power transmission grid and pipeline infrastructures.

Infrastructure	Connectivity cost		Interconnection cost	
	Unit	Value	Unit	Value
Transmission grid[a]	USD/MW	303,554	USD/km	1,182
Pipeline (biomethane)[b]	USD/MW	49,452	USD/km	7,643
Pipeline (steam/heat)[c]	USD/MW	342,520	USD/km	76,955

[a]Adapted based on the parameters from Mesfun et al. [34].

[b]Adapted based on the parameters from Hoo et al. [47].

[c]Adapted based on the parameters from the IEA-ETSAP report [48].

2.3 Availability of bioenergy feedstock

To improve resource efficiency at the national scale, the wastes generated from agricultural production are used as feedstock for bioenergy production. The availability potential of the bioenergy feedstock used in this study is based on the remaining availability of feedstock after subtracting the existing feedstock utilization for energy purposes from the overall availability. The bioenergy feedstock is sourced from three types of agriculture, namely palm oil, paddy, and livestock. From palm oil, the bioenergy feedstock comes from empty fruit bunch (EFB), mesocarp fibre (MF), POME, oil palm frond (OPF) and oil palm trunk (OPT); from paddy, the bioenergy feedstock comes from rice straw (RS) and rice husk (RH); and from livestock, the bioenergy feedstock comes from cattle, buffalo, sheep, goat, chicken and duck manures. Crude palm oil (CPO) is also considered a feedstock for producing palm oil-based biodiesel, but its consumption is limited to up to 16% of the total availability, which is equivalent to providing a substitution for up to 40% of the diesel demand. The availability and the prices of the bioenergy feedstock are provided in Fig. 4. Overall, 280 TWh/year to 330 TWh/year of

agricultural residues are available for utilization from 2020 to 2050, 18 TWh/year to 21 TWh/year of which are dedicated to existing applications (i.e., power and heat). For producing biodiesel, 34 TWh/year to 56 TWh/year of CPO is available for utilization from 2020 to 2050.

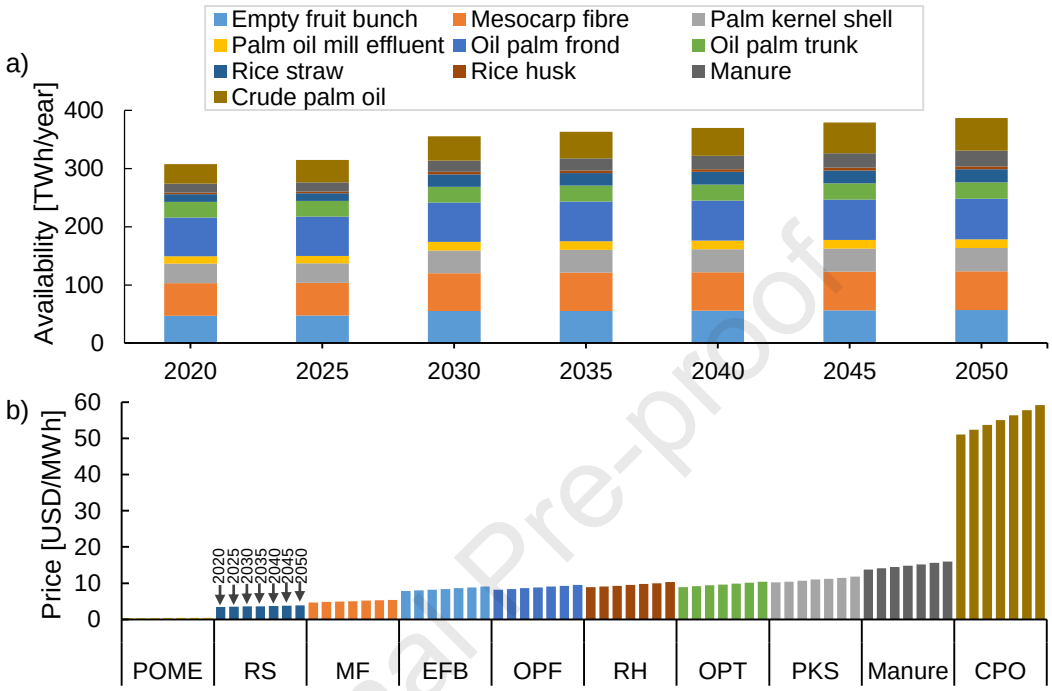

Fig. 4: The types, availabilities, and prices of bioenergy feedstock considered in BeWhere Malaysia, as compiled by Mohd Idris et al. [46]: a) availability of feedstock from 2020–2050, b) price of feedstock from 2020–2050.

The spatially disaggregated bioenergy feedstock availability dataset can be referred to online in the IIASA's data repository [46]. The following assumptions were made for the spatial disaggregation of the bioenergy feedstock availability: the EFB, MF, PKS and CPO availabilities are spatially disaggregated based on the locations and capacities of palm oil mills [51]; OPF and OPT availabilities are spatially disaggregated based on the oil palm plantation map [52]; RH availability is spatially disaggregated based on the locations and capacities of rice mills [51]; RS availability is spatially disaggregated based on the paddy plantation map [53]; and manure availability is spatially disaggregated based on the livestock population map [54].

2.4 Energy demands of the power, heat, and transport sectors

In the model, the energy demands are met by either bioenergy or fossil fuels or by the proportion of bioenergy and fossil fuels. The amount of bioenergy produced in this study is influenced by the amount of energy decarbonization needed to meet the national target. The energy demands in the model are split into three focus sectors, namely power, heat, and transport. For the power sector, the trend of future electricity generation by coal is considered the reference energy demand in the model. Annual increase of 1.48% is assumed to project the annual electricity generation demand from 2020 to 2050 [55]. The share of coal used in the electricity generation demand is then extracted, based on the fuel mix projection for Malaysia [41]. The focus on coal is to emphasize the competition of bioelectricity production from dedicated bioelectricity plants and co-firing plants. For the heat sector, bioheat production as a byproduct from combined heat and power (CHP) technology is considered an option to decarbonize natural gas-based heat in the industries. The annual increase rates of natural gas consumption, determined from the industrial natural gas consumption trend [41], are multiplied with the current rate of natural gas consumed for district injection in the heat sector [56]. For the transport sector, the future diesel and gasoline consumption trends are considered the reference energy demand in the model [41]. The trend of the sectoral energy demands of the power, heat, and transport sectors of Malaysia is illustrated in Fig. 5. Overall, 70 TWh to 155 TWh of coal-based electricity demand, 47 TWh to 74 TWh of gas-based heat demand, and 199 TWh to 330 TWh of oil-based transport fuel demand must be met during the period 2020–2050. Among the fossil fuels considered for meeting the energy demand, coal-based electricity has the highest emission intensity factor at 0.871 tCO_2/TWh [57], followed by diesel-based transport fuel at 0.275 tCO_2/TWh [58], gasoline-based transport fuel at 0.261 tCO_2/TWh [58], and natural gas-based heat at 0.201 tCO_2/TWh [58].

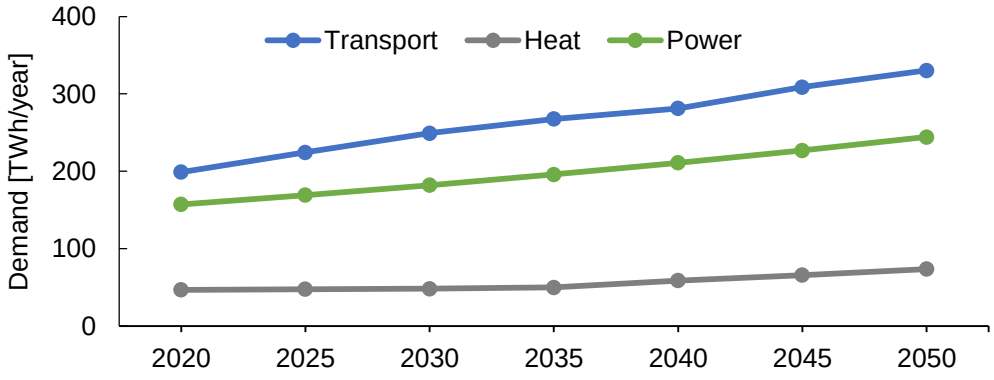

Fig. 5: Sectoral energy demands of the power, heat, and transport sectors of Malaysia [41,55,56].

The spatially disaggregated energy demand dataset can be referred to online in the IIASA's data repository [46]. The following assumptions were made for the spatial disaggregation of the energy demands: electricity demand is spatially disaggregated based on the locations of electricity substations; heat demand is spatially disaggregated based on the locations of natural gas grids; and transport fuel demand is spatially disaggregated based on the population map.

2.5 Bioenergy technologies for promoting multi-sectoral CO_2 reduction

The technologies listed in Table 3 are incorporated in the model as the pre-processing and conversion options in producing bioenergy. The technologies are assumed to be available throughout the planning period of 2020–2050. All the technological deployments in the model are based on the localization of bioenergy facilities in the specific sites, rather than regionally aggregated. Depending on the types of feedstock and technology, biomass feedstock can either directly undergo a main conversion stage for conversion into bioenergy products or undergo a pre-processing stage first, before its final conversion into bioenergy products. Pelletization is included as one of the pre-processing options to take into account the impact of biomass densification in enhancing the energy density of biomass so that the transportation cost can be minimized [50] and the biomass feedstock can be utilized in co-firing application [5]. Other pre-processing options included in the model are biogas upgrading technologies, namely biomethane and BioCNG. These technologies are included to allow the biogas content of raw biogas feedstock (e.g., POME or manure) to be transported over longer distances [47,64]. For the main conversion stage, the technological options considered are based on the bioenergy product types suitable for deployment in the three energy sectors assessed, namely bioelectricity (power sector), bioheat (heat sector), and biodiesel, bioethanol, FT-diesel and FT-gasoline (transport sector).

Co-firing is included as one of the bioenergy technology options in the model to take into account the impact that capital cost savings provided by co-firing have on reducing the overall bioenergy costs. Among the co-firing options (i.e., direct, indirect, and parallel), only direct co-

firing, where the biomass and coal are combusted together in the same boiler to produce steam for electricity production, is included as one of the biomass technologies for producing bioenergy. This consideration was taken because 1) direct co-firing has been widely practiced in most commercial operations [1], making it suitable for deployment in the short run if national policy demands; and 2) other types of co-firing require much more capital investment than direct co-firing, due to the additional infrastructural requirements [59]. For instances, indirect co-firing requires a dedicated gasifier to convert the biomass feedstock into a fuel gas that can be co-combusted with coal, and parallel co-firing requires a dedicated boiler to perform the separate combustion of biomass to produce steam [1]. In the model, the maximum co-firing rate allowed is 20% of the coal plant's generation capacity [5], provided with either pelletized biomass or PKS used as an energy feedstock. The reference energy efficiency, CAPEX, O&M costs, and fuel costs of the coal plants used in the assessment are 38% (based on LHV), 35 USD/MWh_{out}, 9 USD/MWh_{out} and 28–32 USD/MWh_{out}, respectively. More information on each form of bioenergy technology cost can be found in Mohd Idris et al. [46].

Table 3: Relationship between feedstock, technology and product, technology costs and conversion efficiencies of bioenergy technologies implemented in BeWhere Malaysia.

Technology	Input	Output	Efficiency (LHV)	Base CAPEX (USD/kW_{out})	Data sources
Pelletization	EFB, MF, OPF, OPT, RS, RH	Pellet	98%	80	[60-62]
Anaerobic digestor (AD) + water scrubbing	POME, manure	Biomethane	90%	1,050	[63]
AD + water scrubbing + gas bottling	POME, manure	BioCNG	89%	1,100	[63,64]
AD + gas engine	POME, manure	Bioelectricity	34%	2,500	[65,66]
Engine-generator (genset)	BioCNG, Biomethane	Bioelectricity	40%	170	[67]
Fixed bed boiler + steam turbine	EFB, MF, PKS, OPF, OPT, RS, RH, Pellet	Bioelectricity	30%	2,840	[66,68]
CFB boiler + steam turbine (CHP)	EFB, MF, PKS, OPF, OPT, RS, RH, Pellet	Bioelectricity + Bioheat	35% + 50%	4360	[66,69]
Co-milling (co-firing)	PKS, Pellet	Bioelectricity	36%	160	[59]
Gasification + upgrading (Fischer Tropsch (FT)-	EFB, MF, PKS, OPF, OPT, RS, RH,	FT-diesel + FT-gasoline	37% + 12%	2190	[70,71]

synthesis)	Pellet				
Pre-treatment + fermentation (EFB)	EFB	Bioethanol	35%	600	[72]
Pre-treatment + fermentation (OPF)	OPF	Bioethanol	51%	820	[73]
Transesterification	CPO	Biodiesel (Fatty acid methyl ester)	84%	160	[74]

2.6 Scenario description

The national policy adopted for the assessment in this study is related to the achievement of the CO_2 reduction target outlined under the Malaysia's Nationally Determined Contribution (NDC). This is based on the unconditional NDC of the Malaysian energy sector, which committed to a 35% reduction in GHG emission intensity by 2030, compared to the 2005 level [75]. The reason for considering the CO_2 reduction target based on unconditional NDC instead of the overall NDC is to examine whether the current and future availabilities of bioenergy supply would be sufficient to meet the unconditional CO_2 reduction commitment. Extrapolation of the target to 2050 was performed, based on the unconditional CO_2 reduction commitment trend of 2005–2030, to provide the long-term bioenergy development direction. Since the target for 2030–2050 is estimated, uncertainty may arise regarding the future projection of the CO_2 reduction target. To address this uncertainty, alternative CO_2 reduction targets for the period 2030–2050 have been projected, which is based on the maximum rate of the base CO_2 reduction. Preliminary model runs were conducted by increasing the unconditional CO_2 reduction target, extrapolated for 2030-2050, until the maximum value is observed (i.e., at 45% increase of the unconditional CO_2 reduction target) prior to reaching the infeasibility point. This maximal decarbonization target is useful in providing insights into how far the CO_2 reduction commitment in the unconditional NDC can be extended to deliver more ambitious national strategies. The extrapolated CO_2 reduction policy targets are compiled in Fig. 6. Each CO_2 reduction target is employed in the model as a lower bound constraint to be met at various points in the planning period (i.e., 2020, 2025, 2030, 2035, 2040, 2045, and 2050)

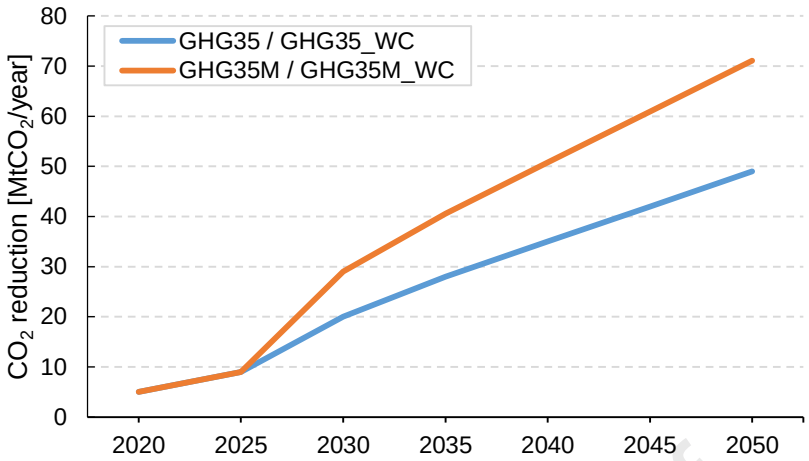

Fig. 6: CO_2 reduction policy targets of the policy scenarios from 2020 to 2050 at a five-year time step.

Several policy scenarios were developed, which include: 1) GHG35—this reflects the deployment of bioenergy (including co-firing) in meeting the unconditional CO_2 reduction target; 2) GHG35_WC—this is a similar scenario to GHG35, but without co-firing as one of the technological options; 3) GHG35M—this reflects the deployment of bioenergy (including co-firing) for meeting the maximal decarbonization target, based on the highest increment of CO_2 reduction relative to the target in GHG35; and 4) GHG35M_WC—this is a similar scenario to GHG35M, but without co-firing as one of the technological options. Throughout the analysis, only the results in 2030 and 2050 are visualized to focus on the comparison of bioenergy deployment, with and without co-firing among the scenarios. The policy scenarios (i.e., GHG35, GHG35_WC, GHG35M, and GHG35_WC) were also run under different supply chain cost parameter variations to analyze the impact of price fluctuations on the technological deployment, biomass utilization and cost reduction potential. These cost parameter sensitivity scenarios are outlined as follows:

1) *Baseline*: The base scenario that acts as the point of comparison with other cost sensitivity scenarios. All policy scenarios are initially run based on this scenario.
2) *+50%_resCost*: The scenario in which all agricultural residue prices increase by 50% (2030-2050).
3) *-50%_resCost*: The scenario in which all agricultural residue prices decrease by 50% (2030-2050).
4) *+50%_cpoCost*: The scenario in which the CPO price increases by 50% (2030-2050).

5) *-50%_cpoCost*: The scenario in which the CPO price decreases by 50% (2030-2050).
6) *+50%_transCost*: The scenario in which the transport costs of commodities increase by 50% (2030-2050).
7) *-50%_transCost*: The scenario in which the transport costs of commodities decrease by 50% (2030-2050).
8) *+50%_capCost*: The scenario in which the investment costs of technologies increase by 50% (2030-2050).
9) *-50%_capCost*: The scenario in which the investment costs of technologies decrease by 50% (2030-2050).
10) *+50%_infraCost*: The scenario in which the investment costs of infrastructures (i.e., grid transmission, pipeline) increase by 50% (2030-2050).
11) *-50%_infraCost*: The scenario in which the investment costs of infrastructures (i.e., grid transmission, pipeline) decrease by 50% (2030-2050).

3.0 Results and discussions

3.1 Reference scenario

Fig. 7 presents the distribution of CO_2 reduction by states in Malaysia during 2030 and 2050 for each policy scenario (Baseline). The resultant CO_2 reduction achieved in each scenario follows the exact minimum bound of CO_2 reduction target expressed in the model, meaning that achieving a higher target than is bounded is not economically feasible. Relative to the unconditional CO_2 reduction commitment in the NDC (i.e., GHG35 and GHG35_WC) in 2030 and 2050, the CO_2 reduction can be maximally extended to 29 $MtCO_2$/year and 71 $MtCO_2$/year, as illustrated in GHG35M and GHG35_WC, the equivalent of a 45% increase from the unconditional targets. The states with coal-fired power plants are Johor (Tanjung Bin), Negeri Sembilan (Jimah), Selangor (Kapar), Perak (Manjung) and Sarawak (Sejingkat, Mukah and Balingian). The contribution of CO_2 reduction by these five states minimizes when co-firing is not allowed. This can be shown as follows: CO_2 reductions in Johor, Perak and Sarawak reduce by 31%, 33% and 72% in 2030, respectively, based on the comparison of GHG35_WC with GHG35; CO_2 reductions in Johor, Negeri Sembilan, Perak and Selangor reduce by 23%, 60%, 41% and 22% in 2050, respectively, based on the comparison of GHG35_WC with GHG35; CO_2

reductions in Johor, Negeri Sembilan, Perak and Sarawak reduce by 18%, 74%, 39% and 24% in 2030, respectively, based on the comparison of GHG35M_WC with GHG35M; and CO_2 reductions in Negeri Sembilan and Selangor reduce by 38% and 4% in 2050, respectively, based on the comparison of GHG35M_WC with GHG35M. The decrease of the CO_2 reduction in these states is accompanied by the increase of the CO_2 reduction in other states. For instance, CO_2 reductions in Penang, Kelantan, Terengganu and Sabah increase by 414%, 13%, 41% and 6% in 2030, respectively, when co-firing is not allowed, based on the comparison of GHG35_WC with GHG35. The highest CO_2 reduction among the states can be observed in Sabah in 2050 and is approximately 16 $MtCO_2$/year, according to the GHG35M and GHG35M_WC scenarios.

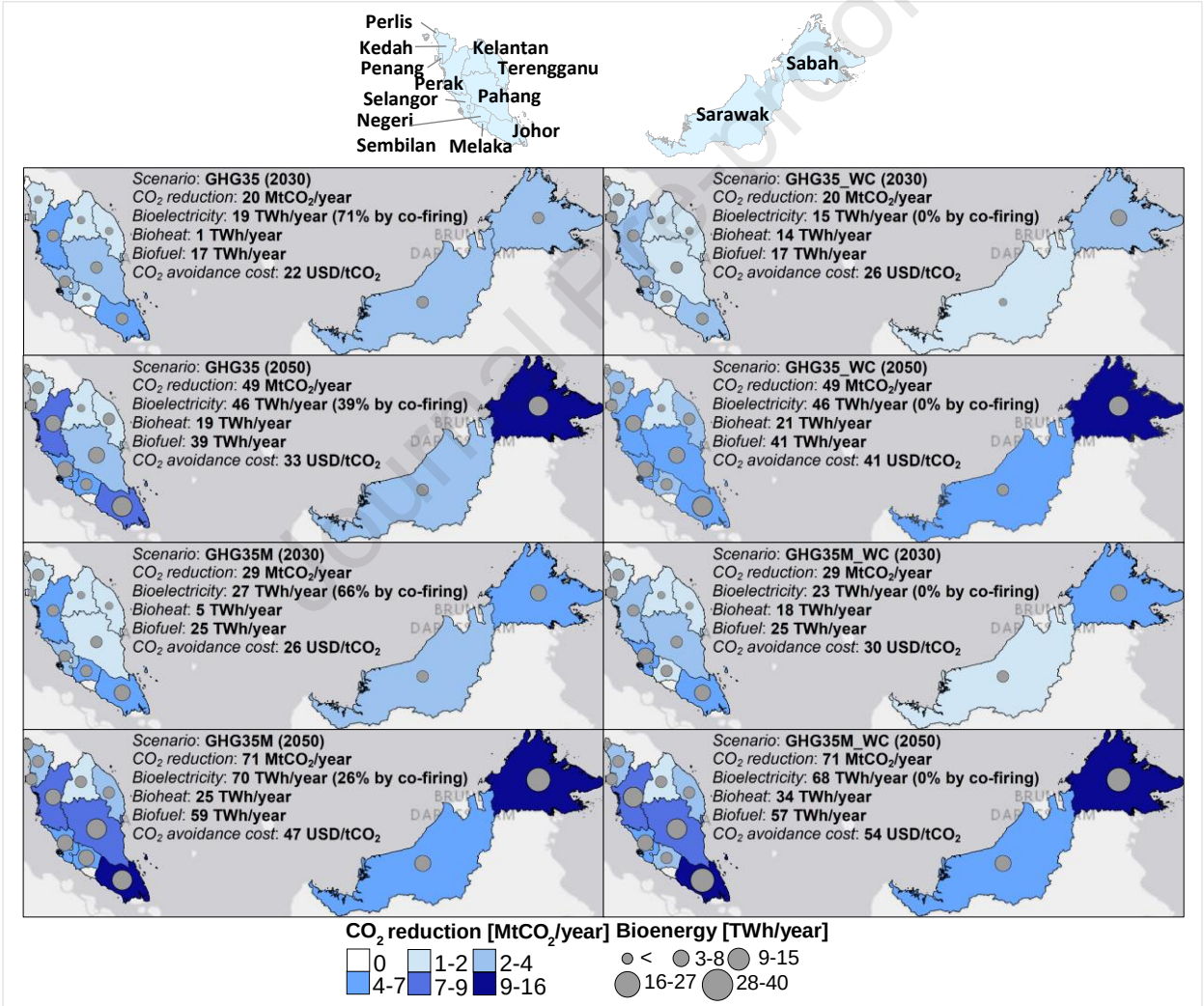

Fig. 7: CO_2 reduction and bioenergy production by each state of Malaysia in the policy scenarios (Baseline).

The co-firing capacities in GHG35 and GHG35M constitute 26–71% of the total bioelectricity produced (see Fig. 7), equivalent to 13–18 TWh/year (see Fig. 8). The unavailability of co-firing increases the production of bioenergy from dedicated bioenergy options, to deliver similar CO_2 reduction as in the scenarios that allow co-firing. This is illustrated in GHG35_WC and GHG35M_WC scenarios, in which the total bioenergy production increases by 3–26% compared to GHG35 and GHG35M, respectively. This is caused by the absence of co-firing that can provide up to 18 TWh/year of bioenergy capacity, causing the shift to dedicated bioenergy production in delivering the CO_2 reduction. In most scenarios, the unavailability of co-firing increases the capacity of specific bioenergy technologies in the bioenergy mix: CHP in 2030, and CHP and fixed bed boilers in 2050. Biofuel production is approximately similar in all scenarios; however, the differences can be noted through the composition of the technologies. While the requirements of dedicated bioenergy production increase in the scenarios that did not include co-firing, the unavailability of co-firing reduces the total feedstock requirements for meeting the CO_2 reduction target by 1-9% in most scenarios. This is caused by the shift to CHP technology, which has a higher energy conversion efficiency (i.e., 85% conversion efficiency) than co-firing (i.e., 36% conversion efficiency), thus reducing the feedstock requirements due to greater efficiency in the conversion of feedstock.

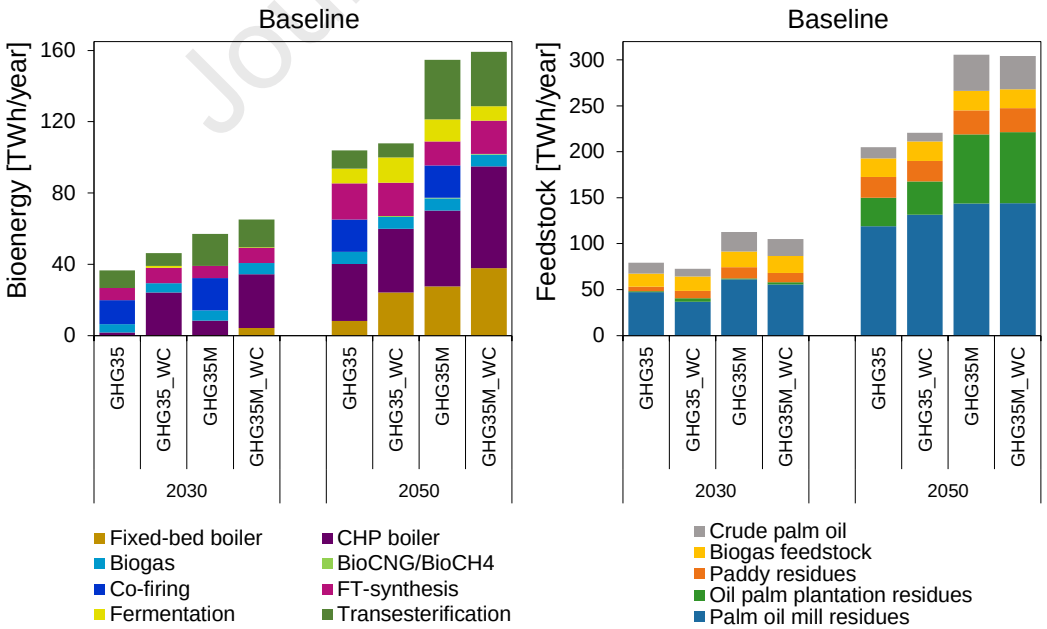

Fig. 8: Technological deployment and feedstock utilization in the policy scenarios (Baseline).

The energy balance of the studied energy production system for each policy scenario can be referred to in Figs. 9 and 10. The efficiencies of biomass feedstock conversion into bioenergy product range from 43% to 64% in 2030 and 49% to 52% in 2050. This may also mean that of the 72–113 TWh/year and 212–306 TWh/year of biomass feedstock supplied in 2030 and 2050, 36–57% and 48–51% (respectively) of the energy converted from biomass cannot be transformed into useful energy forms. The losses of energy occur because of several factors: for bioenergy technologies that deal with thermal processes (e.g., biogas, fixed bed combustion, CHP, co-firing, and gasification), it occurs due to the inability of some proportion of the thermal energy produced to do useful mechanical work (according to the principle underlying the second law of thermodynamics); for other bioenergy technologies, one reason that the loss occurs is the conversion of some proportion of the feedstock into byproducts that are unsuitable to be used for energy purpose, e.g., glycerol generated from biodiesel production [74]. Of the overall feedstock consumed, about 12–30% and 37–51% of them are converted into biomass pellets before their conversion into bioenergy products to fulfill the feedstock demand in co-firing plants and other bioenergy plants (e.g., fixed bed combustion, CHP, and gasification) in 2030 and 2050, respectively. As mentioned previously, pelletization serves at least two purposes in the context of this study: 1) to allow co-firing to be performed at 20% of coal plant capacity, and 2) to allow allocation of feedstock at a lower transport cost. The increase in biomass pellet demand in 2050 is mainly caused by the latter purpose, since more biomass feedstock is needed to meet a higher decarbonization target in 2050, which requires the transportation of these feedstock at a lower cost. Other pre-processing options are also involved to enhance the energy properties of the feedstock, such as biogas upgrading technologies (i.e., biomethane, BioCNG); however, only small proportions of the biogas feedstock are upgraded into biomethane and BioCNG, as shown in Fig. 10. The remaining portions of the overall feedstock consumed (constituting 70–88% and 49–63% of the input biomass in 2030 and 2050, respectively) are allocated to bioenergy plants directly without pre-processing. Looking at the rates of bioenergy deployed in each energy sector in each scenario, it can be observed that the unavailability of co-firing reduces the requirement of bioenergy production in the power sector by up to 22% and 3% in 2030 and 2050, respectively. However, this demands that heat and transport sectors produce more bioenergy to fulfil the overall decarbonization target: the bioenergy requirement in the heat sector increases by up to a factor of 7 in 2030 and by 34% in 2050; the bioenergy requirement in the transport sector

increases by up to 9% in 2030 and 8% in 2050. Overall, percentages of around 21–24%, 3–20% and 18–23% of the overall feedstock consumed are converted into bioenergy in the power, heat and transport sectors, respectively.

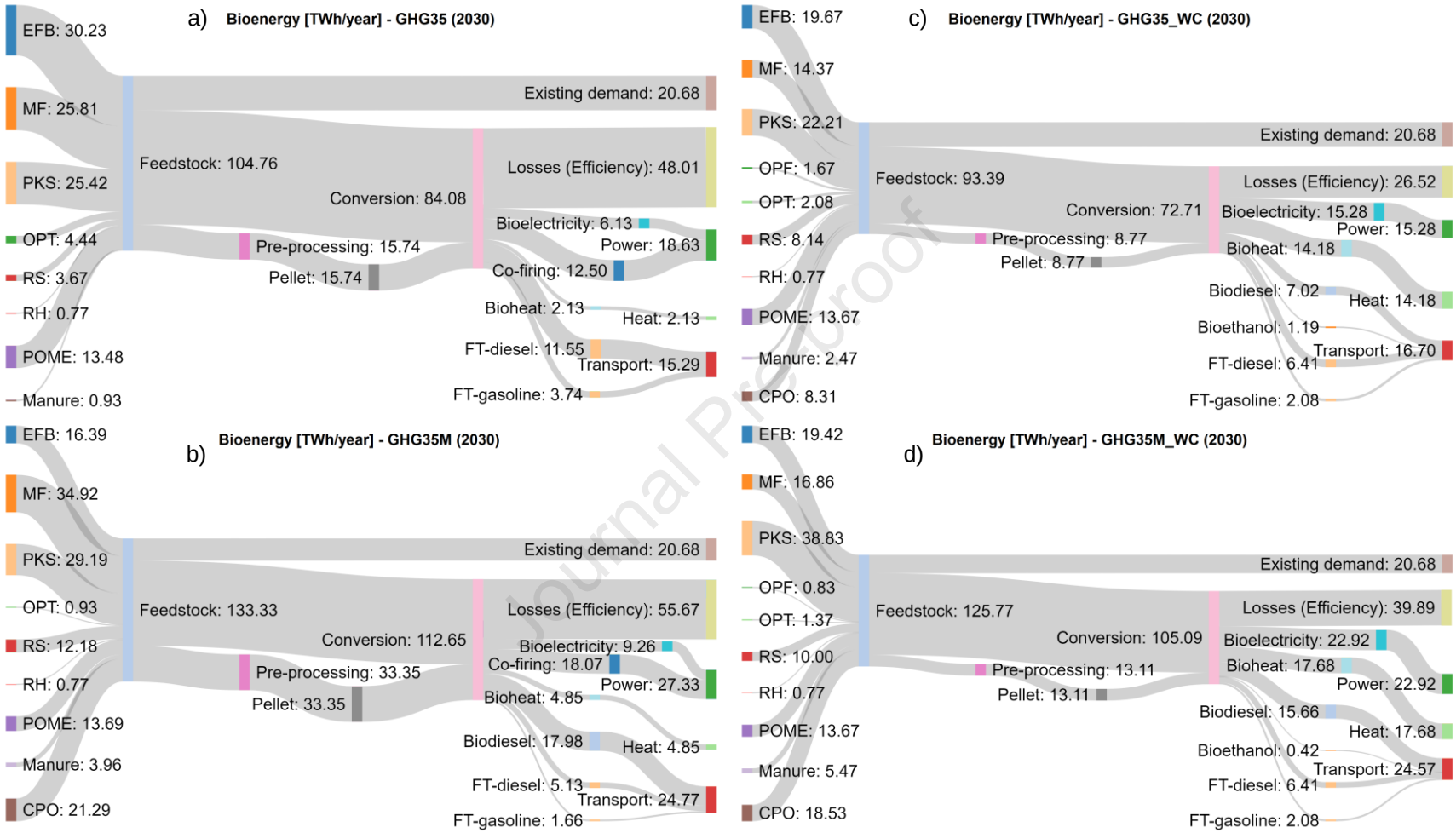

Fig. 9: Flows of bioenergy in 2030 for all policy scenarios: a) GHG35, b) GHG35M, c) GHG35_WC, and d) GHG35M_WC.

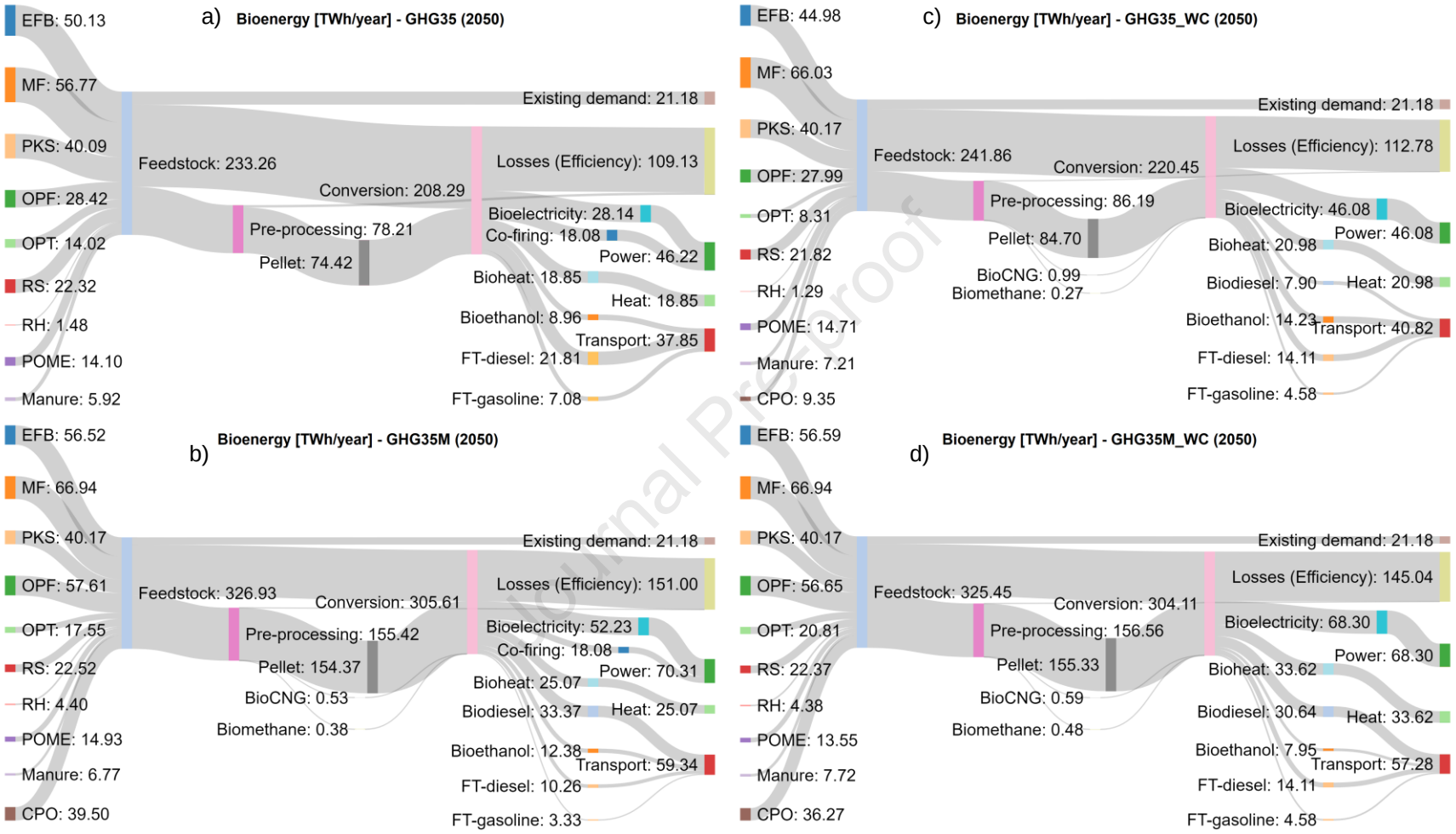

Fig. 10: Flows of bioenergy in 2050 for all policy scenarios: a) GHG35, b) GHG35M, c) GHG35_WC, and d) GHG35M_WC.

The spatially disaggregated representations of the technological deployment are shown in Figs. 11 and 12. It can be observed that the unavailability of co-firing pushes the deployment of dedicated bioelectricity technologies in GHG35_WC and GHG35M_WC, compared to the deployment in GHG35 and GHG35M, respectively. This is shown by the increasing number of bioelectricity plants in GHG35_WC and GHG35M_WC to cater to the unavailability of large-scale co-firing plant capacities. Among the technologies, the most distributed deployment of bioelectricity is shown by biogas. The scattered distribution pattern of biogas plant locations is caused by the difficulty in transporting biogas feedstock such as POME, due to its slurry characteristics, which leads to the onsite application of feedstock in existing mills. In adding a greater biogas capacity, the transformation of most of the existing mills into biogas facilities is preferable than to transport the biogas feedstock to centralized locations for bioelectricity generation. The difficulty in transporting the biogas feedstock can be minimized by converting the feedstock into a denser energy carrier such as biomethane and BioCNG. The conversion of biogas feedstock into BioCNG/biomethane is shown in all the four scenarios; however, only the small-scale deployment of this technology (i.e., total generation of less than 0.5 TWh/year) is economically feasible. As biogas-based technology can only consume specific types of feedstock (e.g., POME, manure), less generation of bioelectricity by this technology is observed relative to other technologies such as CHP and fixed-bed combustion, which can use a wider range of feedstock. For CHP, as most available heat sinks are located in Peninsular Malaysia, its deployment is confined to this region. Due to this reason, to satisfy the electricity demand in Malaysia Borneo, fixed-bed combustion technology is then deployed. As a result, the proportion of bioelectricity by the fixed-bed combustion technology is 51–75% higher in Malaysia Borneo than Peninsular Malaysia in most scenarios. The unavailability of co-firing does not significantly affect the total rate of biofuel being produced in 2050, however, a minor increase of advanced biofuel production (i.e., bioethanol and FT-liquids) relative to biodiesel from CPO can be observed. This is shown by the increase in the total capacities of both advanced biofuel technologies as illustrated in Fig. 12. By comparing the two advanced biofuel technologies, less distributed locations of FT-synthesis technology can be observed than with the fermentation technology due to the larger plant sizes deployed by the former. The higher decarbonization targets in GHG35M and GHG35M_WC contribute to the dominative share of palm oil-based biodiesel as a proportion of the total biofuel produced. This is due to the limited amount of

feedstock from agricultural residues available at the maximum decarbonization target, which pushes the deployment of transesterification technology that does not consume agricultural residues to deliver the remaining CO_2 reduction commitment. For this reason, a more distributed facility configuration of palm oil-based biodiesel is observed in GHG35M and GHG35M_WC than with other biofuel technologies, to purposely increase production to meet the demand.

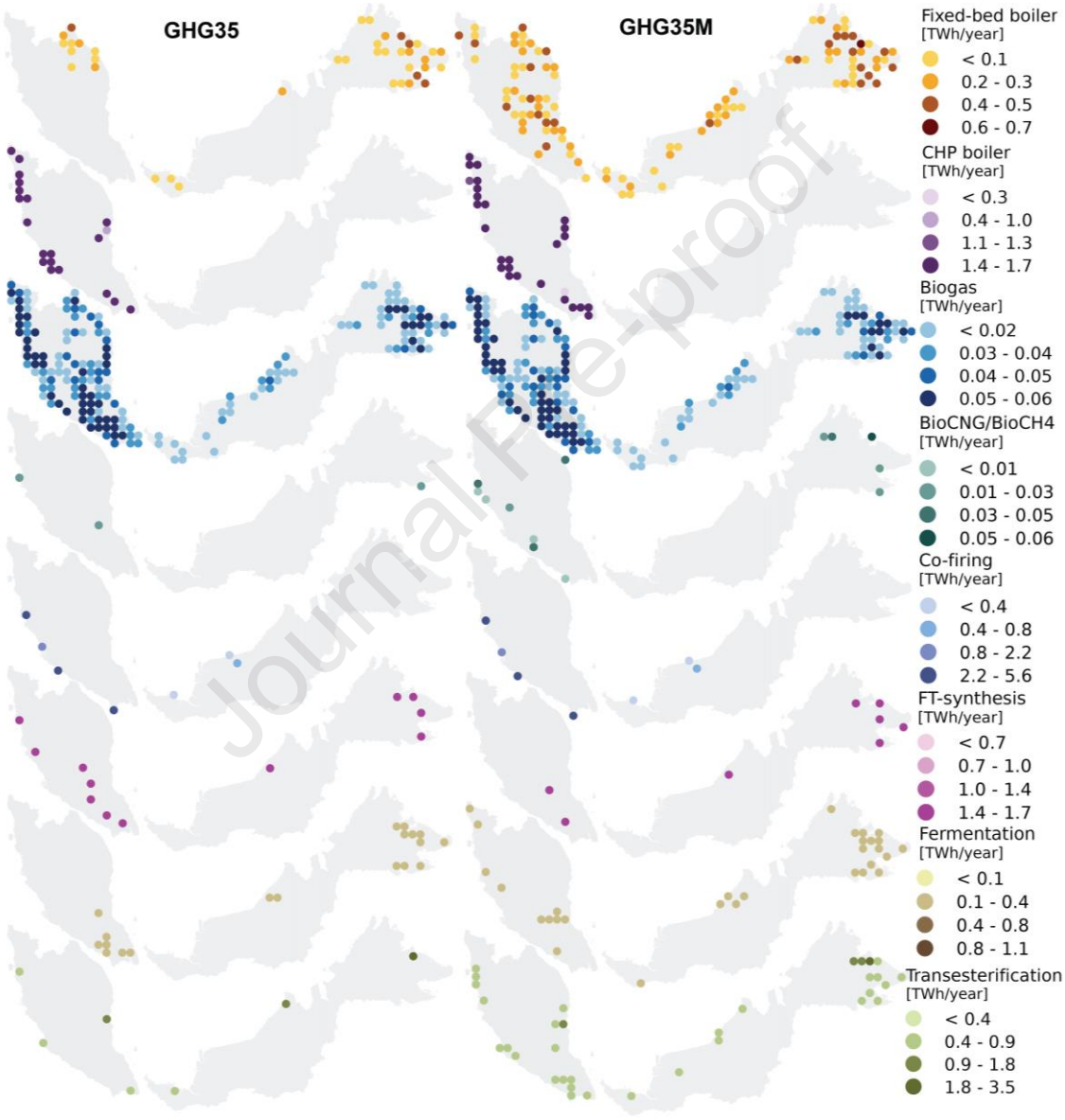

Fig. 11: Spatial distribution of bioenergy technologies (with co-firing) in 2050 in the GHG35 and GHG35M scenarios (Baseline).

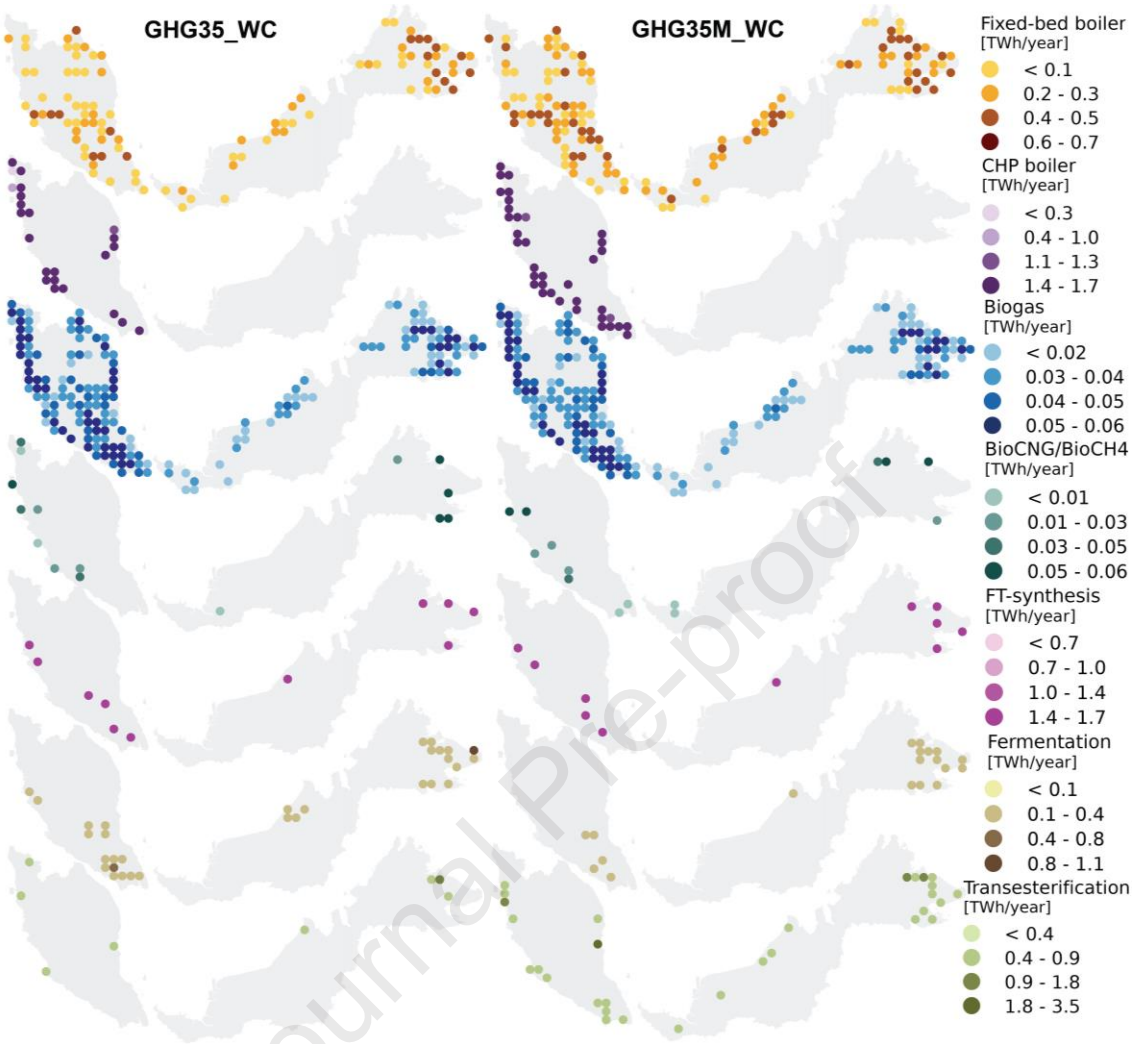

Fig. 12: Spatial distribution of the bioenergy technologies (without co-firing) in the 2050 in GHG35_WC and GHG35M_WC scenario (Baseline).

To deliver the unconditional decarbonization commitment in 2030 and 2050, CO_2 avoidance cost of 22 USD/tCO_2 and 33 USD/tCO_2 would be needed, respectively (see Fig. 7). The rise in CO_2 avoidance cost from 2030 to 2050 is caused by the increase in the commitment of CO_2 to be reduced. If the deployment of co-firing is not allowed, the CO_2 avoidance costs in 2030 and 2050 increase to 26 USD/tCO_2 and 41 USD/tCO_2, respectively, which are 19% and 27% higher relative to the scenarios in which co-firing is allowed. In the scenarios in which decarbonization commitments in 2030 and 2050 are increased to their maximum values (i.e., in GHG35M and GHG35M_WC), the CO_2 avoidance costs increase by 18% and 47% compared to the costs in GHG35 and GHG35_WC, respectively. The increase in the costs of deploying

bioenergy without the contribution of co-firing indicates the opportunity for cost reduction while still meeting the decarbonization targets.

3.2 Cost parameter sensitivity scenarios

The robustness of bioenergy production (Fig. 13), feedstock consumption (Fig. 14), power transmission infrastructure requirement (Fig. 15) and cost reduction potential (Fig. 16) compared to Baseline were assessed based on alternative runs of the policy scenarios (i.e., GHG35, GHG35_WC, GHG35M, and GHG35M_WC) under the impact of increasing CO_2 reduction targets and supply chain cost parameter variations. In almost all the cases where the cost parameters are varied, the increase and the decrease in values of the variables mentioned (i.e., bioenergy, feedstock, infrastructure, and cost) can be observed from the figures, illustrating the sensitivity of the cost parameter variations to the main findings in the Baseline scenario. It can also be suggested that the cost parameter variations do not hinder the selection of co-firing as one of the main bioenergy options for delivering the energy demand in meeting the decarbonization targets. To conveniently convey the key messages that can be extracted from the complex trends illustrated in the figures, several key insights other than noted in the previous section (e.g., the unavailability of co-firing reduces the contribution of CO_2 emission reduction in most of the states where coal-fired power plants are located (Fig. 7), the unavailability of co-firing pushes dedicated bioelectricity technology deployment (Fig. 8), large-scale bioenergy production requires transformation of agricultural mills into energy-producing facilities (Figs. 11 and 12)) are summarized in the following paragraphs.

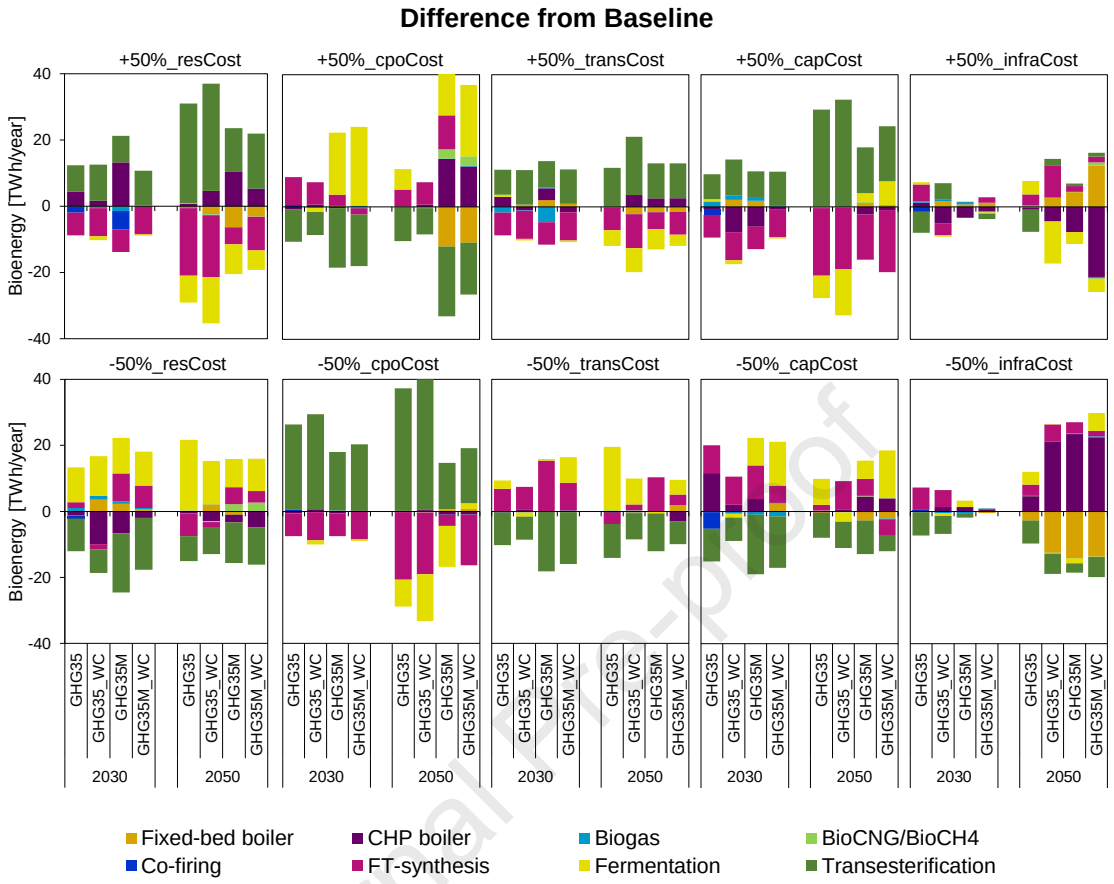

Fig. 13: Technology mix of bioenergy production in the policy scenarios under the impact of increasing CO_2 reduction targets and supply chain cost parameter variations.

An increase in majority of agricultural residues-related costs drives the production of biodiesel from crude palm oil while decreasing the production of advanced biofuels. This insight is illustrated in the three cost parameter sensitivity scenarios, namely +50%_resCost, +50%_transCost and +50%_capCost. These scenarios show approximately similar increases in biodiesel production and decreases in advanced biofuel production in 2030 across the main policy scenarios, at ranges of 8–11 TWh/year and 6–10 TWh/year, respectively. However, after the demand of bioenergy rises in 2050, the scenario in which the transport cost is increased (+50%_transCost) illustrates the minimal rise in biodiesel production and decline in advanced biofuel production across the main policy scenarios, at ranges of 11–18 TWh/year and 10–17 TWh/year, respectively. Both +50%_resCost and +50%_capCost show approximately similar increases in biodiesel production and decreases in advanced biofuel production in 2050 across the

main policy scenarios, at ranges of 13–32 TWh/year and 11–33 TWh/year, respectively. Conversely, in -50%_resCost, -50%_transCost and -50%_capCost, the trends show that the decrease in most agricultural residues-related costs drives the production of advanced biofuel while decreasing the production of biodiesel from CPO.

An increase in crude palm oil-related costs decreases the production of biodiesel while driving the production of advanced biofuel. This insight is illustrated in +50%_cpoCost, which involves a decrease in biodiesel production (see Fig. 13) and CPO utilization (see Fig. 14). All the decreases in 2030 illustrate the zero production of biodiesel in meeting the decarbonization targets. Biodiesel production only appears in 2050 in GHG35M and GHG35M_WC (which is relatively lesser than the biodiesel produced in the Baseline) after most of the residues have been utilized in meeting the maximal decarbonization commitment. Conversely, in -50%_cpoCost, the trend shows that a decrease in CPO-related costs drives biodiesel production while decreasing the production of advanced biofuel. In this scenario, 40% of palm oil biodiesel mix (B40), which was set as a maximum blending mix for biodiesel in the model, is met in all policy scenarios (i.e., GHG35, GHG35_WC, GHG35M, and GHG35M_WC). B40 is equivalent to 36 TWh/year and 47 TWh/year of biodiesel production in 2030 and 2050, respectively.

A decrease in infrastructure-related costs drives the deployment of combined heat and power technologies while reducing the requirement for standalone bioelectricity technology. In the model, infrastructures are treated as transport modes associated with delivering products from one location to another. The infrastructure types considered in the model include power transmission line, biomethane pipelines and steam pipelines (CHP). Decreases in the costs of these infrastructures significantly drive the deployment of CHP, as shown in -50%_infraCost. Conversely, the increase in the infrastructure cost drives the deployment of standalone bioelectricity technology, such as fixed-bed boilers, while reducing the CHP capacity, as shown in +50%_infraCost. Since CHP is associated with both power transmission lines and steam pipelines to distribute (respectively) bioelectricity and bioheat to the demands and has a higher energy efficiency, the reduction in infrastructure costs in -50%_infraCost promotes a preference for this technology over dedicated bioelectricity

technology (i.e., fixed-bed boiler) in delivering the bioelectricity requirements (after fulfillment by biogas and co-firing) to meet the decarbonization target. Meeting the unconditional and maximal decarbonization commitments in GHG35 and GHG35M would mean maximum CHP capacities of 37 TWh/year and 66 TWh/year, respectively, would be deployed in 2050. The unavailability of co-firing significantly pushes for maximum CHP capacities higher by 55% (57 TWh/year) and 21% (80 TWh/year) in 2050, as shown in GHG35_WC and GHG35M_WC, respectively. Overall, in each policy scenario (i.e., GHG35, GHG35_WC, GHG35M, and GHG35M_WC), -50%_infraCost shows the highest rate of CHP capacity being deployed in 2050 compared to the rates in other cost parameter sensitivity scenarios.

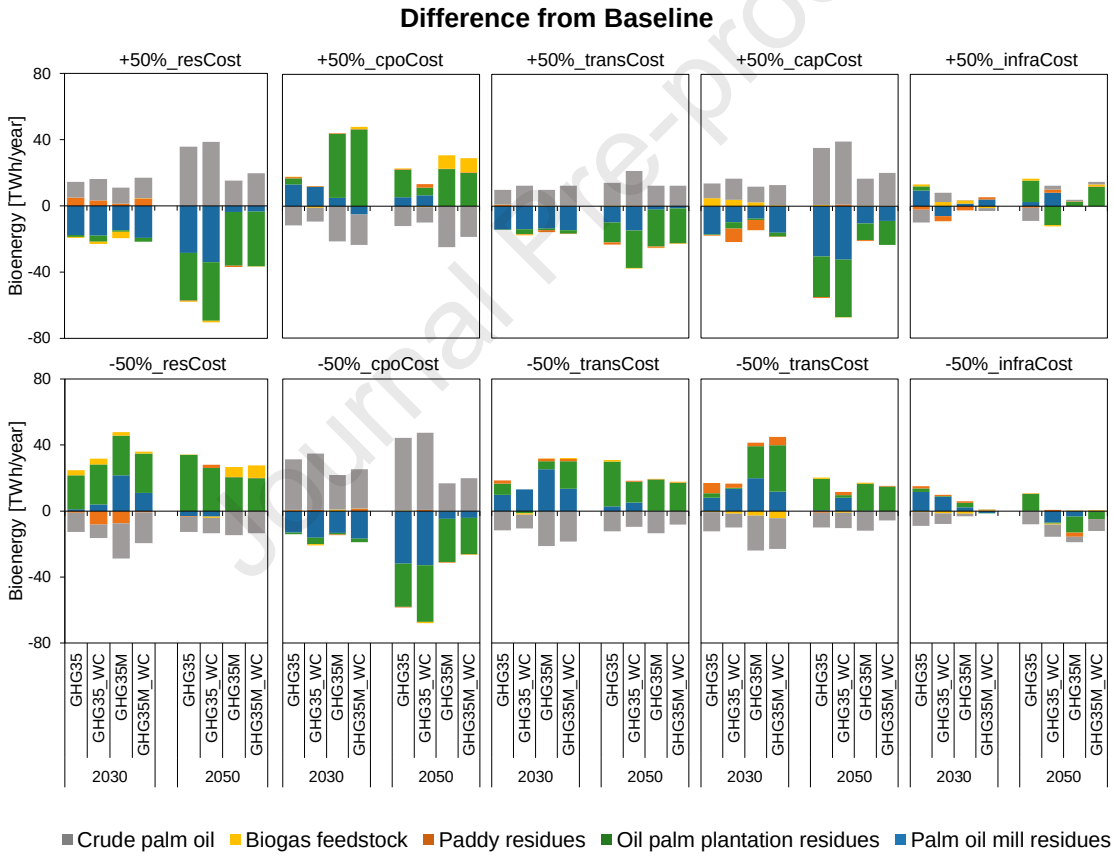

Fig. 14: Feedstock utilization in the policy scenarios under the impact of increasing CO_2 reduction targets and supply chain cost parameter variations.

An increase in bioelectricity production demands a larger extension of power transmission infrastructure from existing agricultural mills to electricity substations. As illustrated in Fig. 8, in the Baseline, production of bioelectricity across all policy scenarios (i.e., GHG35, GHG35_WC, GHG35M, and GHG35M_WC) increases significantly from 2030 to 2050 by a factor of up to 3. Due to the variations in the values of the cost parameters (see Fig. 13), bioelectricity production rates fluctuate from the Baseline but only in the range of -4 TWh/year to 4 TWh/year. Thus, each policy scenario's power transmission requirements (i.e., GHG35, GHG35_WC, GHG35M, and GHG35M_WC) in the Baseline vary insignificantly, relative to the majority of the other cost parameter sensitivity scenarios (see Fig. 15). However, if compared based on the planning periods, it can be observed that the power transmission requirements in all policy scenarios in 2050 increase significantly relative to 2030, as shown in Fig. 13, due to the increase in bioelectricity production (see Figs. 8 and 13). The maximum power transmission requirement rises sequentially from 2030 to 2050, from an average of 24 GWkm in 2030 to 56 GWkm (GHG35), 127 GWkm (GHG35_WC), 184 GWkm (GHG35M) and 254 GWkm (GHG35M_WC) in 2050, following the order of which the total amount of bioelectricity produced from dedicated bioelectricity technologies increases from the lowest to the highest (see Figs. 8 and 13). This trend highlights that the unavailability of co-firing (presented by GHG35_WC and GHG35M_WC) contributes to a larger extension of power transmission requirements relative to when co-firing is available (presented by GHG35 and GHG35M). This is because, when co-firing is unavailable, more deployment of dedicated bioelectricity technologies is needed to meet the decarbonization target (see Fig. 13), contributing to a greater infrastructure requirement for bioelectricity transmission. When co-firing is available, less infrastructure is needed as co-firing uses the existing transmission infrastructure of coal plants to distribute bioelectricity.

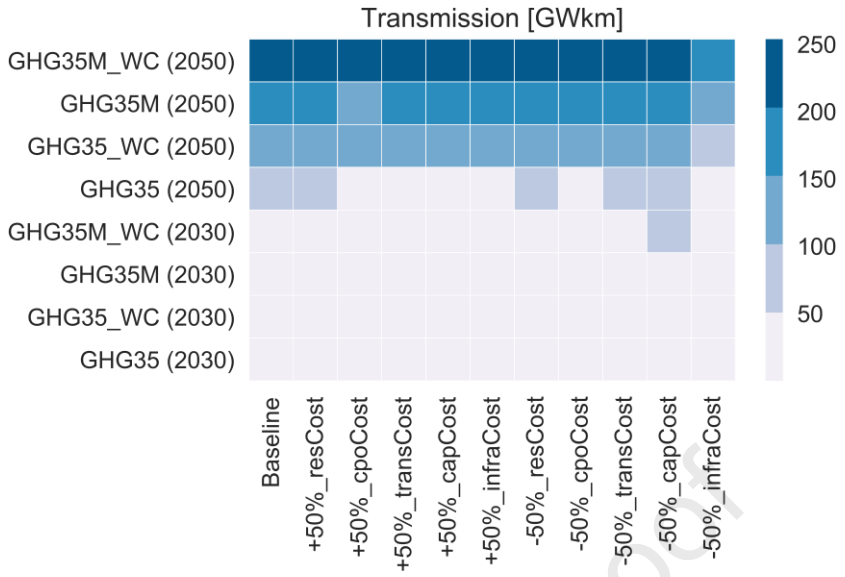

Fig. 15: Power transmission infrastructure requirements in the policy scenarios under the impact of increasing CO_2 reduction targets and supply chain cost parameter variations. The values reflect the multiplication of the bioelectricity transmission capacity and the extension distance of the power transmission line from the existing palm oil/rice mills to the electricity substations.

The costs of meeting decarbonization goals are mostly impacted by the changes to the feedstock-related costs and the technology investment costs. This insight is shown in Fig. 16, which illustrates the impact of supply chain cost parameter variations on the CO_2 avoidance costs of meeting different energy decarbonization targets. The reduction in the CO_2 avoidance costs is illustrated in the cases where the cost parameter values of the selected supply chain cost elements (i.e., agricultural residues price, CPO price, transport cost, capital cost, and infrastructure cost) are reduced to half of their baseline values. It is evident that the cost reduction declines with the increasing level of ambition of the decarbonization target in most of these cases. These declines are contributed by several notable factors, such as 1) the increase in the transport cost due to the need to mobilize more biomass (see Figs. 8 and 14) in meeting growing bioenergy demand (see Figs. 8 and 13) to achieve higher decarbonization targets; 2) the increase in the infrastructure costs due to the greater infrastructures required to meet growing bioelectricity and bioheat demands (see Figs. 8 and 13); and 3) the increase in the technology costs due to the increased requirements to deploy more expensive technologies after the available capacities of less expensive technologies have been fully, or almost fully, utilized (see Table 3, Fig. 8 and Fig. 13). Among the cost parameter variations, the greatest reduction in the CO_2 avoidance costs—up

to 183% of cost reduction—is evident when the price of CPO is halved, as shown in -50%_cpoCost. The dominance of the CPO price in significantly contributing to the decrease in the CO_2 avoidance costs is due to the base CPO prices used in the Baseline, which are relatively higher than the prices of the other biomass feedstocks (see Fig. 4). The decrease in the CPO price then pushes the dominance of biodiesel from CPO in the bioenergy mix—to up to 65% of the overall bioenergy produced (see Figs. 8 and 13)—to meet the decarbonization targets. This dominance is also contributed by 1) transesterification technology, which has the highest conversion efficiency relative to other main conversion technologies (see Table 3); 2) the absence of competition in CPO utilization by other conversion technologies (see Table 3); and 3) the absence of a requirement for CPO to be sent to pre-processing plant before conversion into biodiesel (see Table 3). Examining the case where the price of CPO increases by half (+50%_cpoCost), it can be observed that the increase in the CPO price does not significantly increase the CO_2 avoidance costs in the same way that the CO_2 avoidance costs are largely reduced when the price of CPO decreases. This is because CPO is no longer cost-effective to be utilized in +50%_cpoCost, so the priority is given to utilize the remaining agricultural residues available, which have significantly lower prices than CPO. Because of this priority, a decline in the CPO requirement (in most policy scenarios, no CPO utilization can be observed) and a rise in the agricultural residues requirement can be observed in +50%_cpoCost, as illustrated in Fig. 14. Other cases involving the impact of feedstock price changes on increasing or decreasing the CO_2 avoidance costs are illustrated in +50%_resCost and -50%_resCost. Because almost all the bioenergy technologies considered in the model (except transesterification) are dependent on agricultural residues to produce bioenergy, it is evident that an increase in the price of agricultural residues (i.e., +50%_resCost) means a higher rise in costs than an increase in the CPO price (i.e., +50%_cpoCost). In +50%_resCost, increases of up to 42% and 38% in the CO_2 avoidance costs can be illustrated in 2030 and 2050, respectively; in +50%_cpoCost, increases of up to 15% and 23% of the CO_2 avoidance costs can be shown in 2030 and 2050, respectively. In +50%_cpoCost, the system has a choice to fully eliminate CPO utilization in most of the policy scenarios so that it need not bear the high cost of CPO to produce bioenergy (see Fig. 14). However, in +50%_resCost, the system has no choice but to depend on agricultural residues to produce bioenergy because the full utilization of the available CPO allowed for consumption is insufficient to solely deliver the required energy decarbonization (see Figs. 4 and 14).

Meanwhile, a decrease in the price of agricultural residues (i.e., -50%_resCost) reduces the CO_2 avoidance costs by up to 67% in 2030 and 49% in 2050, which are lower than the cost reduction rates in the cases where the CPO price decreases (i.e., -50%_cpoCost). These lower cost reduction rates are directly contributed by the agricultural residues prices, which are significantly lower than the CPO price. Aside from the CPO price, another parameter significantly contributing to the cost of meeting decarbonization target is the technology capital cost. The results show that capital cost has a strong influence in both increases and decreases in the CO_2 avoidance costs. It can be observed that the CO_2 avoidance cost rise is the highest in those cases where the capital cost of technology increases by half (i.e., +50%_capCost). This illustrates increases in CO_2 avoidance costs of up to 96% and 81% in 2030 and 2050, respectively. Since all technologies are required to pay for capital costs in order to be deployed, even technology that is retrofitted in the existing fossil fuel assets (see Table 3), the increases in the CO_2 avoidance costs are unavoidable when the input capital cost parameter for each technology is increased. The results also show the dominance of capital cost in reducing the overall costs of meeting decarbonization targets. When the technology capital cost is reduced by half (i.e., -50%_capCost), cost reductions of up to 139% and 94% can be observed in 2030 and 2050, respectively. The 2030 cost reduction in -50%_capCost, even though lower than the cost reduction in -50%_cpoCost, is still relatively higher than the cost reduction rates in all other cost parameter sensitivity cases (i.e., -50%_resCost, -50%_transCost, -50%_infraCost). The strong influence of capital cost in reducing the CO_2 avoidance costs is further shown in 2050, when a decrease in the technology capital cost contributes to the highest cost reduction among other cost parameter changes.

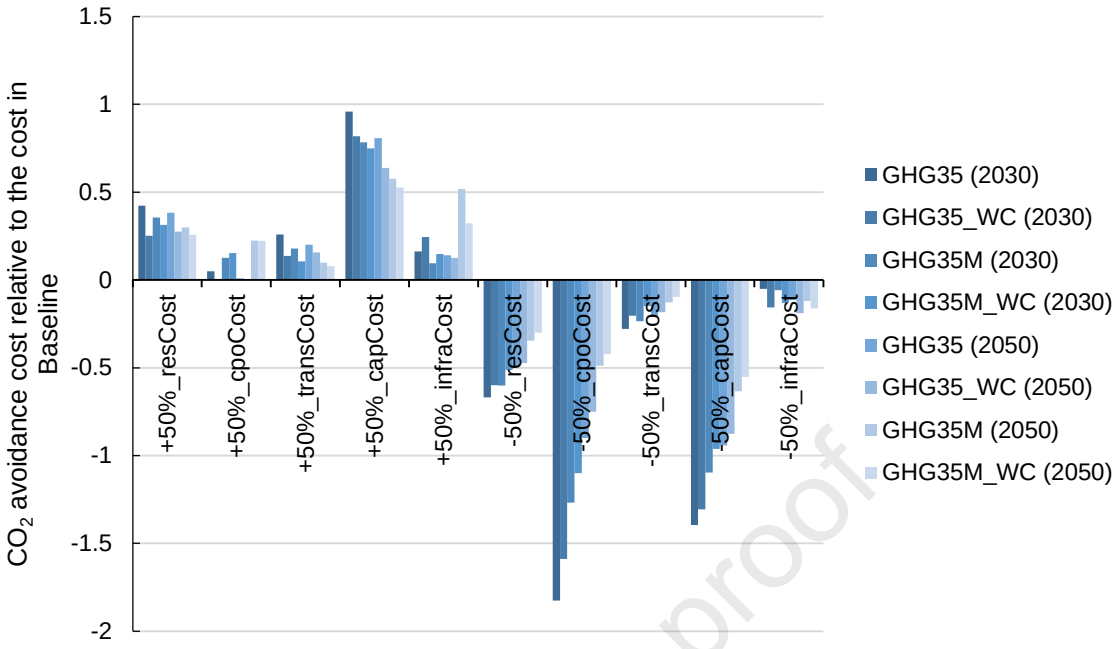

Fig. 16: CO_2 avoidance costs relative to the CO_2 avoidance costs in Baseline (Fig. 7) under the impact of increasing CO_2 reduction targets and supply chain cost parameters variations.

Transformation of coal plants into co-firing reduces the bioenergy cost of meeting decarbonization goals. To meet the target set in the Paris Agreement, Malaysia needs to deliver a substantial amount of CO_2 reduction in its energy sectors. Bioenergy can play a key role in contributing to the achievement of this target, based on the opportunity to mobilize the agricultural wastes generated from large-scale agricultural production in the country. Despite this promising potential, the current bioenergy capacity that has been deployed in the Malaysian energy sectors is still low; e.g., the total amount of renewable energy deployed in the power sector (including bioenergy) constitutes only about 2% of the energy mix [76]. Co-firing can offer a cost-effective strategy in the short term to stimulate large-scale bioenergy capacity deployment. By simultaneously deploying co-firing with dedicated biomass technologies, significant capital cost savings can be made, reducing the overall bioenergy cost to meet the energy decarbonization targets. This insight is illustrated in Fig. 17, where the CO_2 avoidance costs of bioenergy in scenarios that do not allow co-firing (i.e., GHG35_WC and GHG35M_WC) are higher than the those in scenarios that allow co-firing (i.e., GHG35, GHG35M). In the Baseline, it is clear that the CO_2 avoidance costs required to meet the unconditional decarbonization targets in 2030 and 2050 can be respectively reduced by up to 19% and 27%

when co-firing is allowed as shown in GHG35. The increase in the commitment to decarbonize energy sectors in GHG35M has caused the cost reduction potential to decrease to 15% in both planning years (i.e., 2030 and 2050). This decrease is contributed by the drop in the share of co-firing as part of the total bioenergy capacity deployed in GHG35M, owing to the increase of bioenergy production from dedicated biomass technologies to deliver more CO_2 reduction; this reduces the capital cost saving potential that can be provided by co-firing. As expected, the uses of higher and lower values (±50%) of supply chain cost parameters in the model cause, respectively, a decline and rise in the CO_2 avoidance cost reduction in most cost parameter sensitivity cases. There is a notable difference worth highlighting - almost all cases involving an increase in the cost parameter values show a moderate reduction of the cost reduction potential in the Baseline; however, certain scenarios involving a decrease in the cost parameter values show extreme increases in the cost reduction potentials, as illustrated, for example, in -50%_cpoCost and -50%_capCost. It can be deduced from Fig. 17 that the two dominant parameters contributing to the highest increase in the cost reduction potential are CPO price (-50%_cpoCost) and capital cost (-50%_capCost). The cost reduction potential can be enhanced to up to 57% in 2030 and 215% in 2050 in cases where the CPO price reduces by half (i.e., -50%_cpoCost) and to up to 147% in 2030 and 171% in 2050 in cases where the technology capital cost reduces by half (i.e., -50%_capCost). Other cost parameters also have a significant impact on increasing the cost reduction potential: increases of up to 44% and 31% of the cost reduction potential can be observed in -50%_resCost and -50%_transCost, respectively. The degree to which the cost reduction potential rises (shown in Fig. 17) is similar to the degree to which the CO_2 avoidance costs fall according to the decrease in the supply chain cost parameter values (shown in Fig. 16). In both cases, increases in the cost reduction potential are observed in the following order: the highest cost reduction is shown in -50%_cpoCost, followed by -50%_capCost, -50%_resCost, -50%_transCost, and -50%_infraCost. Increases in the cost reduction potentials to rates higher than 100%, as shown in -50%_cpoCost and -50%_capCost, indicate that capital cost savings provided by the deployment of co-firing could result in the improved profitability of the bioenergy system while delivering the decarbonization commitment, but only if the overall supply chain cost is drastically reduced.

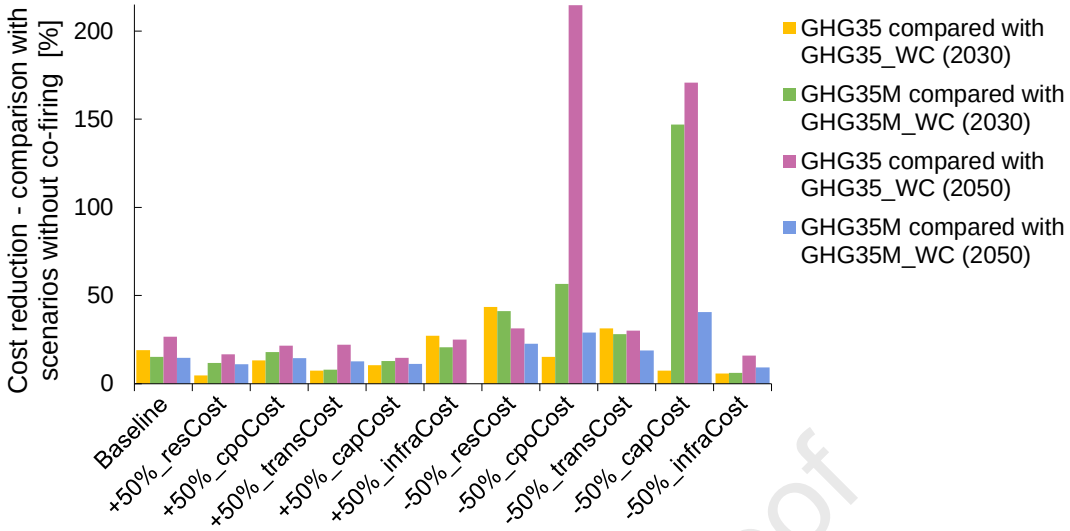

Fig. 17: Cost reduction potential under the impact of increasing CO_2 reduction targets and supply chain cost parameters variations.

4.0 Conclusion

The findings in this study confirm that the deployment of co-firing with dedicated biomass technologies would significantly reduce the bioenergy costs of meeting the decarbonization targets. The rates at which cost reduction can be largely brought are heavily influenced by the minimization of the supply chain cost parameter values. However, even with no the decrease in the overall supply chain cost, up to 27% of CO_2 avoidance cost can be reduced if co-firing is deployed alongside other bioenergy options. This cost reduction is contributed by co-firing, which has a notably lower investment cost than other bioenergy options and higher conversion efficiency than the standalone bioelectricity plants. Nevertheless, co-firing deployment is restricted by the maximum substitution rate allowed in the displacement of a proportion of coal-based electricity generation with bioelectricity. The findings have shown that feasible capacity for co-firing deployment would be reached in the near term, allowing other technological options to fill up the remaining bioenergy capacity needed to deliver the decarbonization in the long term.

The minimization of certain cost parameters can significantly maximize the cost reduction potential. The baseline cost reduction potential could increase to up to 31%, 44%, 171% and

215% if the transport cost, residue price, capital cost and CPO price are reduced by half, respectively. This indicates that feedstock-related and technology-related costs are the most sensitive parameters for defining the cost reduction potentials. This finding shows that particular action should be taken to achieve a reduction in the overall supply chain cost by specifying the focus sectors for improvement. However, this also shows that the trade-off between other economic sectors should be considered in future studies, as this might enable the greatest benefit to be provided at a national level. For instance, the decrease in the CPO price could bring economic and environmental benefit to the energy sector by delivering decarbonization through a profitable biodiesel production. However, this could negatively impact the economic sector in terms of the agricultural contribution to GDP if CPO price is significantly lowered, as this feedstock is extremely protectable as a high-value commodity. Actions to minimize the cost of specific supply chain elements should thus be regarded as short-term challenges to be undertaken by developing countries with rich agricultural resources, such as Malaysia.

Specifically, the ranges of which CO_2 reduction commitment of the NDC can be extended beyond 2030 have been investigated in the case of Malaysia. This study finds that up to 45% of the CO_2 reduction commitments for the period 2030–2050 can be increased relative to the unconditional CO_2 reduction commitment based from the contribution that can be made by bioenergy. The minimum and maximum ranges of CO_2 reduction required during the period 2030–2050 are 20–49 $MtCO_2$/year and 29–71 $MtCO_2$/year, respectively. This finding will be useful as a point of comparison with future studies that focus on the NDC implementation beyond 2030 in the energy sector of Malaysia.

The significant reductions in bioenergy costs enabled by the availability of fossil fuel substitution technology (i.e., co-firing) and the decrease in feedstock price, transport cost, investment cost, and infrastructure cost highlight that choices of feedstock, transport and technology are crucial in delivering decarbonization. This confirms the need for range of decision-making options before actions are finalized. The application of a spatio-temporal techno-economic optimization model in this study can, therefore, be justified as a tool for generating a number of insights for informing policies and supply chain planning. The insights outlined in this work open the door for future opportunities for similar analysis across energy

sectors and scales to identify unique synergies between bioenergy policy analysis and techno-economic assessment conducted at various spatial and temporal scales.

Acknowledgements

This article has been supported by the "Sustainable Bioeconomy Futures" project, which is internally funded by the International Institute for Applied Systems Analysis, the BECOOL project under the European Union's Horizon 2020 Research and Innovation Programme (grant agreement No. 744821), Universiti Teknologi Malaysia for providing additional research funds under Vote No. Q.J130000.2409.08G96.

References

[1] Roni M.S., Chowdhury S., Mamun S., Marufuzzaman M., Lein W., Johnson S., 2017, Biomass co-firing technology with policies, challenges, and opportunities: A global review, Renewable and Sustainable Energy Reviews, 78, 1089-1101.

[2] Keller V., Benjamin L., Jeffrey E., Taco N., Kevin P.W., Iman M., Bryson R., Peter W., Andrew R., 2018, Coal-to-biomass retrofit in Alberta–value of forest residue bioenergy in the electricity system, Renewable Energy, 125, 373-383.

[3] Cutz L., Berndes G., Johnsson F., 2019, A techno- economic assessment of biomass co-firing in Czech Republic, France, Germany and Poland, Biofuels, Bioproducts and Biorefining, 13(5), 1289-1305.

[4] Knapp S., Güldemund A., Weyand S., Schebek L., 2019, Evaluation of co-firing as a cost-effective short-term sustainable CO_2 mitigation strategy in Germany, Energy, Sustainability and Society, 9(1), 32.

[5] Khorshidi Z., Ho M.T., Wiley D.E., 2014, The impact of biomass quality and quantity on the performance and economics of co-firing plants with and without CO2 capture, International Journal of Greenhouse Gas Control, 21, 191–202.

[6] Bhave A., Taylor R.H., Fennell P., Livingston W.R., Shah N., Mac Dowell N., Dennis J., Kraft M., Pourkashanian M., Insa M., Jones J., 2017, Screening and techno-economic assessment of biomass-based power generation with CCS technologies to meet 2050 CO2 targets, Applied Energy, 190, 481–489.

[7] Bui M., Zhang D., Fajardy M., Mac Dowell N., 2021, Delivering carbon negative electricity, heat and hydrogen with BECCS–Comparing the options, International Journal of Hydrogen Energy, https://doi.org/10.1016/j.ijhydene.2021.02.042

[8] Xu Y., Yang K., Zhou J., Zhao G., 2020, Coal-biomass co-firing power generation technology: Current status, challenges and policy implications, Sustainability, 12(9), 3692.

[9] Yang B., Wei Y.M., Liu L.C., Hou Y.B., Zhang K., Yang L., Feng Y., 2021, Life cycle cost assessment of biomass co-firing power plants with CO2 capture and storage considering multiple incentives, Energy Economics, 96, 105173.

[10] Lu Y., Khan Z.A., Alvarez-Alvarado M.S., Zhang Y., Huang Z., Imran M., 2020, A critical review of sustainable energy policies for the promotion of renewable energy sources, Sustainability, 12(12), 5078.

[11] Sun K., Xiao H., Liu S., You S., Yang F., Dong Y., Wang W., Liu Y., 2020. A review of clean electricity policies—From countries to utilities, Sustainability, 12(19), 7946.

[12] Soltani S., Mahmoudi S.M.S., Yari M., Morosuk T., Rosen M.A., Zare V., 2013, A comparative exergoeconomic analysis of two biomass and co-firing combined power plants, Energy Conversion and Management, 76, 83–91.

[13] Malek A.A., Hasanuzzaman M., Abd Rahim N., Al Turki Y.A., 2017, Techno-economic analysis and environmental impact assessment of a 10 MW biomass-based power plant in Malaysia, Journal of cleaner production, 141, 502-513.

[14] Schipfer F., Kranzl L., 2019, Techno-economic evaluation of biomass-to-end-use chains based on densified bioenergy carriers (dBECs), Applied Energy, 239, 715-724.

[15] Clare A., Gou Y.Q., Barnes A., Shackley S., Smallman T.L., Wang W., Jiang D., Li J., 2016, Should China subsidize cofiring to meet its 2020 bioenergy target? A spatio-techno- economic analysis, GCB Bioenergy, 8(3), 550-560.

[16] Aviso K.B., Sy C.L., Tan R.R., Ubando A.T., 2020, Fuzzy optimization of carbon management networks based on direct and indirect biomass co-firing, Renewable and Sustainable Energy Reviews, 132, 110035.

[17] Wang R., Chang S., Cui X., Li J., Ma L., Kumar A., Nie Y., Cai W., 2021, Retrofitting coal- fired power plants with biomass co- firing and carbon capture and storage for net

zero carbon emission: A plant- by- plant assessment framework, GCB Bioenergy, 13(1), 143-160.

[18] Zhou H.L., Silveira S., Tang B.J., Qu S., 2021, Optimal timing for carbon capture retrofitting in biomass-coal combined heat and power plants in China, Journal of Cleaner Production, 293, 126134.

[19] Li J., Wang R., Li H., Nie Y., Song X., Li M., Shi M., Zheng X., Cai W., Wang C., 2021, Unit-level cost-benefit analysis for coal power plants retrofitted with biomass co-firing at a national level by combined GIS and life cycle assessment, Applied Energy, 285, 116494.

[20] Welfle A., Thornley P., Röder M., 2020, A review of the role of bioenergy modelling in renewable energy research & policy development, Biomass and Bioenergy, 136, 105542.

[21] Akgül, A., & Seckiner, S. U., 2019, Optimization of biomass to bioenergy supply chain with tri-generation and district heating and cooling network systems, Computers & Industrial Engineering, 137, 106017.

[22] Roni M.S., Thompson D.N., Hartley D.S., 2019, Distributed biomass supply chain cost optimization to evaluate multiple feedstocks for a biorefinery, Applied Energy, 254, 113660.

[23] Haji Esmaeili S.A., Szmerekovsky J., Sobhani A., Dybing A., Peterson T.O., 2020, Sustainable biomass supply chain network design with biomass switching incentives for first-generation bioethanol producers, Energy policy, 138, 111222.

[24] He-Lambert L., English B.C., Lambert D.M., Shylo O., Larson J.A., Yu T.E., Wilson B., 2018, Determining a geographic high resolution supply chain network for a large scale biofuel industry, Applied Energy, 218, 266-281.

[25] Ng R.T., Kurniawan D., Wang H., Mariska B., Wu W., Maravelias C.T., 2018, Integrated framework for designing spatially explicit biofuel supply chains, Applied Energy, 216, 116-131.

[26] Khanali M., Akram A., Behzadi J., Mostashari-Rad F., Saber Z., Chau K.W., Nabavi-Pelesaraei A., 2021, Multi-objective optimization of energy use and environmental emissions for walnut production using imperialist competitive algorithm, Applied Energy, 284, 116342.

[27] Maheshwari P., Singla S., Shastri Y., 2017, Resiliency optimization of biomass to biofuel supply chain incorporating regional biomass pre-processing depots, Biomass and Bioenergy, 97, 116-131.

[28] Harahap F., Leduc S., Mesfun S., Khatiwada D., Kraxner F., Silveira S., 2019, Opportunities to optimize the palm oil supply chain in Sumatra, Indonesia, Energies, 12(3), 420.

[29] Harahap F., Leduc S., Mesfun S., Khatiwada D., Kraxner F., Silveira S., 2020, Meeting the bioenergy targets from palm oil based biorefineries: An optimal configuration in Indonesia, Applied Energy, 278.

[30] de Jong S., Hoefnagels R., Wetterlund E., Pettersson K., Faaij A., Junginger M., 2017, Cost optimization of biofuel production–The impact of scale, integration, transport and supply chain configurations, Applied Energy, 195, 1055-1070.

[31] Truong A.H., Patrizio P., Leduc S., Kraxner F., Ha-Duong M., 2019, Reducing emissions of the fast growing Vietnamese coal sector: the chances offered by biomass co-firing, Journal of Cleaner Production, 215, 1301-1311.

[32] Nwachukwu, C. M., Wang, C., & Wetterlund, E. (2021). Exploring the role of forest biomass in abating fossil CO2 emissions in the iron and steel industry–The case of Sweden. Applied Energy, 288, 116558.

[33] Mandova H., Leduc S., Wang C., Wetterlund E., Patrizio P., Gale W., Kraxner F., 2018, Possibilities for CO_2 emission reduction using biomass in European integrated steel plants, Biomass and Bioenergy, 115, 231-243.

[34] Mesfun S., Leduc S., Patrizio P., Wetterlund E., Mendoza-Ponce A., Lammens T., Staritsky I., Elbersen B., Lundgren J., Kraxner F., 2018, Spatio-temporal assessment of integrating intermittent electricity in the EU and Western Balkans power sector under ambitious CO_2 emission policies, Energy, 164, 676-693.

[35] Mandova H., Patrizio P., Leduc S., Kjärstad J., Wang C., Wetterlund E., Kraxner F., Gale W., 2019, Achieving carbon-neutral iron and steelmaking in Europe through the deployment of bioenergy with carbon capture and storage, Journal of Cleaner Production, 218, 118-129.

[36] Ascenso L., d'Amore F., Carvalho A., Bezzo F., 2018, Assessing multiple biomass-feedstock in the optimization of power and fuel supply chains for sustainable mobility, Chemical Engineering Research and Design, 131, 127-143.

[37] Sharma B., Brandt C., McCullough- Amal D., Langholtz M., Webb E., 2020, Assessment of the feedstock supply for siting single- and multiple- feedstock biorefineries in the USA and identification of prevalent feedstocks, Biofuels, Bioproducts and Biorefining, 14(3), 578-593.

[38] Durusut E., Tahir F., Foster S., Dineen D., Clancy M., 2018, BioHEAT: A policy decision support tool in Ireland's bioenergy and heat sectors, Applied Energy, 213, 306-321.

[39] Clancy, J. M., Curtis, J., & Ó'Gallachóir, B. (2018). Modelling national policy making to promote bioenergy in heat, transport and electricity to 2030–Interactions, impacts and conflicts. Energy Policy, 123, 579-593.

[40] Patrizio P., Leduc S., Kraxner F., Fuss S., Kindermann G., Mesfun S., Spokas K., Mendoza, A., Mac Dowell N., Wetterlund E., Lundgren J., 2018, Reducing US coal emissions can boost employment, Joule, 2(12), 2633-2648.

[41] IEA, 2015, Southeast Asia energy outlook – World energy outlook special report, International Energy Agency, Paris, France.

[42] Iskandar, M. J., Baharum, A., Anuar, F. H., & Othaman, R. (2018). Palm oil industry in South East Asia and the effluent treatment technology—A review. Environmental technology & innovation, 9, 169-185.

[43] Mohd Idris M.N., Leduc S., Yowargana P., Hashim H., Kraxner F., 2021, Spatio-temporal assessment of the impact of intensive palm oil-based bioenergy deployment on cross-sectoral energy decarbonization, Applied Energy, 285, 116460.

[44] Leduc S., Schwab D., Dotzauer E., Schmid E., Obersteiner M., 2008, Optimal location of wood gasification plants for methanol production with heat recovery, International Journal of Energy Research, 32(12), 1080-1091.

[45] Leduc S. Lundgren J., Franklin O., Dotzauer E., 2010, Location of a biomass based methanol production plant: A dynamic problem in northern Sweden. Applied Energy, 87 (1), 68-75.

[46] Mohd Idris M.N.M., Leduc S., Yowargana P., Kraxner F., 2020, Datasets and mathematical formulation of the BeWhere Malaysia model, https://dare.iiasa.ac.at/108/.

[47] Hoo P.Y., Hashim H., Ho W.S., 2018, Opportunities and challenges: Landfill gas to biomethane injection into natural gas distribution grid through pipeline, Journal of Cleaner Production, 175, 409-419.

[48] IEA-ETSAP, 2013, Technology Brief E16 – District heating, IEA-ETSAP Energy Technology Systems Analysis, Paris, France.

[49] How B.S., Tan K.Y., Lam H.L., 2016, Transportation decision tool for optimisation of integrated biomass flow with vehicle capacity constraints, Journal of Cleaner Production, 136, 197-223.

[50] Rentizelas A.A., Li J., 2016, Techno-economic and carbon emissions analysis of biomass torrefaction downstream in international bioenergy supply chains for co-firing, Energy, 114, 129-142.

[51] SIRIM, 2014, MYREMap, SIRIM Environmental Technology Research Centre, https://gisportal.sirim.my/.

[52] Petersen R., Aksenov D., Esipova E., Goldman E., Harris N., Kuksina N., Kurakina I., Loboda T., Manisha A., Sargent S., Shevade V., 2015, Mapping tree plantations with multispectral imagery: Preliminary results for seven tropical countries, World Resources Institute and Transparent World, Washington, DC.

[53] Nelson A., Gumma M.K., 2015, A map of lowland rice extent in the major rice growing countries of Asia, International Rice Research Institute, Laguna, Philippines, http://irri.org/our-work/research/policy-and-markets/mapping/. [Accessed 15.01.2019].

[54] Gilbert M., Nicolas G., Cinardi G., Boeckel T.P.V., Vanvambeke S.O., Wint G.R.W., Robinson T.P., 2018, Global distribution data for cattle, buffaloes, horses, sheep, goats, pigs, chickens and ducks in 2010, Scientific Data, 5, 180227.

[55] ST, 2017a, Peninsular Malaysia electricity supply outlook, Suruhanjaya Tenaga, Putrajaya, Malaysia.

[56] ST, 2017b, Piped gas distribution industry statistics, Suruhanjaya Tenaga, Putrajaya, Malaysia.

[57] Reddy B.R., Vinu R., 2016, Microwave assisted pyrolysis of Indian and Indonesian coals and product characterization, Fuel Processing Technology, 154, 96-103.

[58] EPA, 2018, Emission factors for greenhouse gas inventories, United States Environmental Protection Agency, DC, United States.

[59] IEA-ETSAP-IRENA, 2013, Technology-Policy Brief E21 – Biomass co-firing in coal power plants, IEA-ETSAP Energy Technology Systems Analysis, Paris, France.

[60] Adams P.W.R., Shirley, J.E.J., McManus M.C., 2015, Comparative cradle-to-gate life cycle assessment of wood pellet production with torrefaction, Applied Energy, 138, 367-380.

[61] Batidzirai B., Mignot A.P.R., Schakel W.B., Junginger H.M., Faaij A.P.C., 2013, Biomass torrefaction technology: Techno-economic status and future prospects, Energy, 62, 196-214.

[62] Agar D.A., 2017, A comparative economic analysis of torrefied pellet production based on state-of-the-art pellets, Biomass and Bioenergy, 97, 155-161.

[63] Rotunno P., Lanzini A., Leone P., 2017, Energy and economic analysis of a water scrubbing based biogas upgrading process for biomethane injection into the gas grid or use as transportation fuel, Renewable Energy, 102, 417-432.

[64] Lee M.K., Hashim H., Lim J.S., Taib M.R., 2019, Spatial planning and optimisation for virtual distribution of BioCNG derived from palm oil mill effluent to meet industrial energy demand, Renewable Energy, 141, 526-540.

[65] MPOB-NKEA, 2013, National Biogas Implementation (EPP5) - Biogas capture and CDM project implementation for palm oil mills, National Key Economic Areas, Selangor, Malaysia.

[66] IRENA, 2018, Renewable power generation costs in 2017, International Renewable Energy Agency, Abu Dhabi, UAE.

[67] Cigala C., 2016, Sustainable Energy Handbook. Module 6.1: Simplified Financial Models, MWH Global, Colorado, United States.

[68] Paulo H., Azcue X., Barbosa-Póvoa A.P., Relvas S., 2015, Supply chain optimization of residual forestry biomass for bioenergy production: The case study of Portugal, Biomass and Bioenergy, 83, 245-256.

[69] S2biom, 2017, Tools for biomass chains, S2biom, http://S2biom-test.alterra.wur.nl/web/guest/bio2match. [Accessed 14.03.2019].

[70] Dimitriou I., Goldingay H., Bridgwater A.V., 2018, Techno-economic and uncertainty analysis of Biomass to Liquid (BTL) systems for transport fuel production, Renewable and Sustainable Energy Reviews, 88, 160-175.

[71] Hagberg, M.B., Pettersson, K., Ahlgren, E.O., 2016, Bioenergy futures in Sweden – Modeling integration scenarios for biofuel production, Energy, 109, 1026-1039.

[72] Quintero J.A., Moncada J., Cardona C.A., 2013, Techno-economic analysis of bioethanol production from lignocellulosic residues in Colombia: A process simulation approach, Bioresource Technology, 139, 300-307.

[73] Abdullah S.S.B.S, 2015, Efficient bioethanol production from oil palm frond petiole, PhD Thesis, Kyushu Institute of Technology, Kitakyushu, Japan.

[74] Harahap F., Silveira S., Khatiwada D., 2019, Cost competitiveness of palm oil biodiesel production in Indonesia, Energy, 170, 62-72.

[75] MESTECC, 2018, Third national communication and second biennial update report to the UNFCCC, Ministry of Energy, Science, Technology, Environment and Climate Change Malaysia, Putrajaya, Malaysia.

[76] IEA. World energy balance 2020. Paris, France: International Energy Agency; 2020.

Highlights

- Biomass co-firing plays an important role in delivering energy decarbonization
- Multi-sectoral deployment helps to improve bioenergy production efficiency
- More bioenergy investments are needed when co-firing is unavailable
- The capital cost savings provided by co-firing reduce energy decarbonization costs
- Changes in supply chain cost parameter values affect the cost reduction potential

Declaration of interests

☒ The authors declare that they have no known competing financial interests or personal relationships that could have appeared to influence the work reported in this paper.

☐The authors declare the following financial interests/personal relationships which may be considered as potential competing interests: